

CASCADE REACTION BASED FLUORESCENT PROBE FOR DETECTION OF HYDROGEN SULFIDE

Thesis submitted towards the partial fulfillment
of BS-MS dual degree programme



by

Pratyush Kumar Mishra

20101092

Under the guidance of

Dr. Pinaki Talukdar

Assistant Professor,

Department of Chemistry

Indian Institute Of Science Education and Research Pune

Certificate

This is to certify that this dissertation entitled “**Cascade reaction based fluorescent probe for detection of hydrogen sulfide.**” towards the partial fulfillment of the BS-MS dual degree programme at the Indian Institute of Science Education and Research, Pune represents original research carried out by “**Pratyush Kumar Mishra** at IISER Pune” under the supervision of “**Dr. Pinaki Talukdar**, assistant Professor, Department of Chemistry” during the academic year 2014-2015.



Dr. Pinaki Talukdar
Assistant Professor
Department of Chemistry
IISER Pune

Declaration

I hereby declare that the matter embodied in the report entitled “**Cascade reaction based fluorescent probe for detection of hydrogen sulfide**” are the results of the investigations carried out by me at the Department of Chemistry, Indian Institute of Science Education and Research Pune, under the supervision of Dr. Pinaki Talukdar and the same has not been submitted elsewhere for any other degree.

Date of Submission: 25-03-2015

Place: Pune

A handwritten signature in black ink that reads "Pratyush". The signature is written in a cursive style with a horizontal line underneath the name.

Pratyush Kumar Mishra

Acknowledgement

I would take this opportunity to express my deep sense of gratitude to my respected guide and mentor, Dr. Pinaki Talukdar for his invaluable guidance, unwavering encouragement, careful nurturing and commitment to go beyond the path of necessity; that have contributed greatly to my development, and without which I could never have successfully culminated the project.

I would like to thank Dnyaneshwar Kand who taught me the techniques and skills of the laboratory which I would cherish for the rest of my life.

I thank all my lab mates Sharad, Dinesh, Arundhati, Tanmoy, Sopan, Sanjit, Javid and Manjeet for their help and making my study at the department pleasant and enjoyable.

I would like to thank my friends for their support throughout my study.

Lastly I would like to give a big hug of thanks out to my parents, whose unwavering faith, love and patience have been like pillars of strength.

Contents

| | |
|--|-----------|
| 1. Abstract | 6 |
| 2. Introduction | |
| i. Fluorescent probes | 7 |
| ii. Background and significance of Hydrogen sulfide | 8 |
| 3. Objective | 14 |
| 3. Materials and Methods | |
| General methods | 16 |
| Physical measurements | 16 |
| Photophysical measurements | 17 |
| Experimental procedure | 17 |
| 4. Results and discussion | 22 |
| 5. Conclusion | 33 |
| 6. References | 34 |
| 7. Appendix | 37 |

Note: Cell imaging studies were carried out by Mr. Tanmoy Saha and crystal data was solved by Mr. Kiran Reddy.

Abstract

Hydrogen sulfide is an essential gasotransmitter that controls several physiological and pathological functions such as, cardiovascular protection, antioxidative effects, cell growth regulation, cell signaling, and apoptosis. In recent years, development of fluorescent H₂S probe that work via cascade reaction process, is of great interest. In the present work, we have developed a new probe based on the azide to amine reduction followed by Pinner cyclization to form iminocoumarin as reporter molecule. The probe showed selective response to hydrogen sulfide over other analytes with $t_{1/2} = 6.1$ min, 31-fold fluorescence enhancement and the limit of detection 169 nM. The probe was also permeable through the cell membranes and its application in live cell imaging of H₂S was also demonstrated using HeLa cells.

Introduction

i) Fluorescent probes

Over past few decades, fluorescence-based tools have gained a tremendous attention of researchers in development of more efficient and specific sensing and imaging techniques for application in wide variety of samples. High sensitivity, simplicity, cost effective nature of fluorescent method encouraged researchers to develop synthetic fluorescent probes which can be applicable in biological samples.¹ Therefore various fluorescent probes for the detection of different biorelevant analyte, explosives,² natural gases were developed.

In the design of fluorescent probes, various fluorophores such as quantum dots, metal complexes, organic dye molecules, etc. were used. Among these probes, small organic molecular probes are crucial because of their structural simplicity, easy tenability, low toxicity and versatile applicability. A typical organic molecular probe in general consists of two key domains: (i) a recognition/reaction site for sensing of an analyte, and (ii) a fluorophore to show the detectable response during sensing. Organic fluorophores such as pyrene, coumarin, fluorescein, rhodamine, BODIPY, etc. (Figure 1) are routinely used for the development of fluorescent probes.

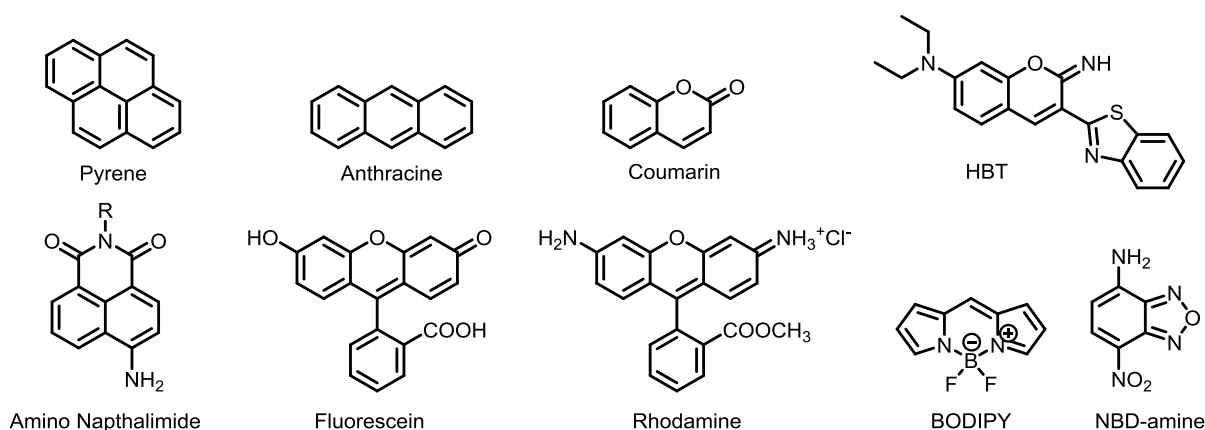


Figure 1. Structures of some routinely used fluorophores.

In terms of sensing mechanism, small molecular organic probes can be classified in two different categories, (i) Chemosensor: sensing mechanism involves non-covalent interaction such as, H-bonding, electrostatic, π - π stacking interactions; and (ii) Chemodosimeter: based on irreversible chemical reaction involving change

in structure by covalent modification.³ Those chemical reaction based probes offers an additional advantages to achieve a great range of analytes with high selectivity because of the huge library of chemical reactions.

On the other hand, by considering the mode of output signal, probes are classified in three major categories, (i) *Turn-On* probe: a non fluorescent molecule converts into fluorescent after reacting with specific analyte; (ii) *Turn-Off* probe: the probe is subjected to quenching of fluorescence intensity after reacting with analyte; and (iii) *Ratiometric* probe: when both probe and reporter molecule exhibit considerable fluorescence intensity but in different wavelength. Among them *Turn-On* probes are always preferable upon *Turn-Off* probes in terms of biological activities. But for monitoring any quantitative transformation or biological pathways, *Ratiometric* probes are always superior than other classes because of their self-calibration⁴ properties. Apart from that an efficient probe should have some general properties such as, high signal to noise ratio⁵, high excitation wavelength, cell permeability, low toxicity and applicability in aqueous media.

ii) **Background and significance of hydrogen sulfide**

Hydrogen sulfide, the volatile and flammable gas, is well known for its pungent smell and noxious nature. Naturally it can be produced from microbial and geological activities. It can also be produced in mammalian cells from Cysteine (Cys) and Homocysteine (Hcy) by the reduction catalyzed by Cystathionine β -synthase⁶ (CBS, mainly localized in brain and liver), Cystathionine γ -lyase⁷ (CSE, mainly localized in liver) and Cysteine aminotransferase / 3-Mercaptopyruvate sulfurtransferase⁸ (CAT/3-MST, mainly localized in vascular endothelium and brain). Recently it was found to be the third most important gaseous signaling molecule in human body after nitric oxide (NO) and carbon monoxide (CO).⁹ Being a gasotransmitter, it controls several physiological and pathological functions such as, cardiovascular protection,^{10,11} antioxidative effects, cell growth regulation,¹² cell signaling,¹³ mediating O₂ sensing in the carotid body¹⁴ and apoptosis.¹⁵ In past few years H₂S releasing molecules are used as prodrugs for treatment of reperfusion injury and inflammatory diseases.¹⁶ But overexposure to the gas or over expression

of H₂S producing enzymes can lead to diseases such as, liver cirrhosis¹⁷, diabetes¹⁸, Alzheimer's disease¹⁹ and Down's syndrome.²⁰

Therefore, to understand the production, mode of action and consumption in biological systems, accurate determination of amount of H₂S is necessary. But because of the volatility, high reactivity and very short life time of this species, determination of amount of H₂S accurately is a challenging interest of researchers. The popular methods were used till date, for the detection of H₂S includes, gas chromatography,²¹ electrochemical²² and colorimetric analysis.²³ However, these methods are not suitable for biological applications because of complex sample preparation, long response time and high detection limit. Therefore, development of fluorescent probes for accurate detection of H₂S in environmental as well as biological samples is a burgeoning field of interest of research.

The popular strategies for development of organic reaction based H₂S probe includes:

1) Nitro to amine reduction: H₂S mediated reduction of nitro to amine leads to a change in electronic properties in structure of probe. A quenched fluorescence state can be achieved by intramolecular charge transfer (ICT) or photoinduced electron transfer (PET) process (Figure 2) by changing the electronic environment of the adjacent group attached to the fluorophore. In the same line, difference in fluorescence properties can be achieved by conversion of nitro group to amine functionality. Fluorescent probes exhibiting a PET mechanism are generally connected to the fluorophore via linker which acts as a sensing moiety and design mechanism works in such a way that either it quenches or enhances the fluorescence. In case of ICT analyte generally alters the electron flow to the fluorophore via conjugated spacer bridge. The probe **1**²⁴ was reported based on the PET mechanism and probes **2-4**²⁵⁻²⁷ were reported to work via the ICT mechanism (Figure 3).

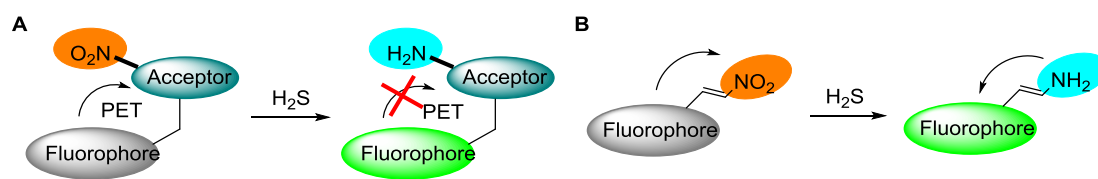


Figure 2. Strategy for fluorescent probe design is based on nitro to amine reduction. Schematic representation of the turn on process based on either a PET (**A**) or ICT (**B**) mechanism in the probe state and destruction of the quenching process after the reaction with H_2S .

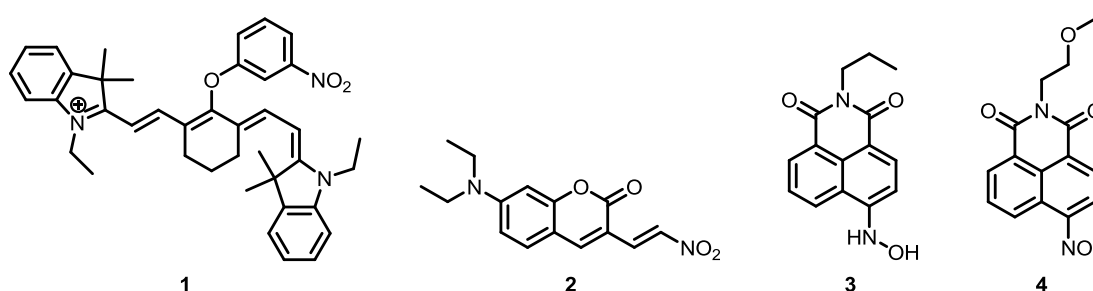


Figure 3. Structures of probes based on nitro to amine reduction.

2) **Selenoxide to selenide reduction:** Organoselenium compounds act as an active site for enzyme glutathione peroxidase. These compounds display antioxidant properties by reacting with reactive oxygen species (ROS). Therefore, various selenoxide to selenide reduction based probes **5-7**^{28,29} were reported exploiting the electron withdrawing nature of selenoxide and donating nature of selenide.

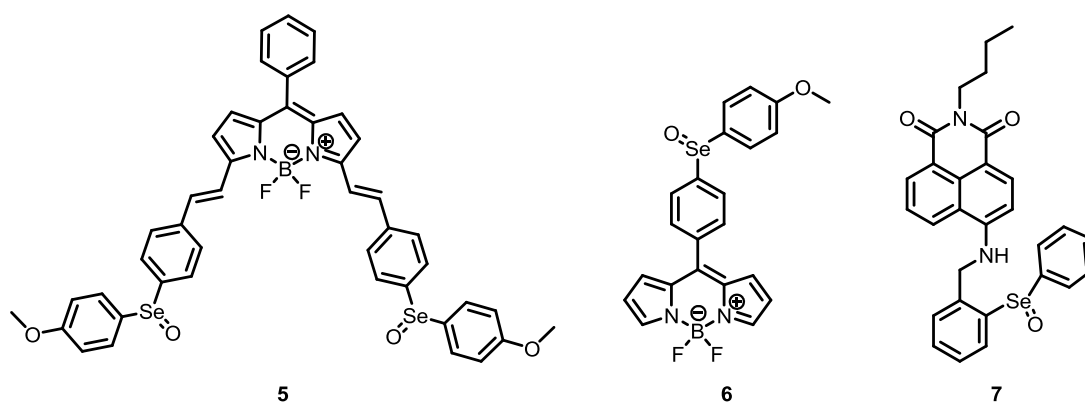


Figure 4. Structures of probes based on selenoxide to selenide reduction.

3) Nucleophilic addition cyclization by H₂S: H₂S has the pK_a of ~ 7 at physiological environment which is lesser than Cys (pK_a ~ 8.3) and GSH (pK_a ~ 9.2). This feature enables H₂S as a better nucleophile compared to other thiols at physiological pH. H₂S can also hold the unique characteristics of dual nucleophilic reactions whereas substituted thiols (such as, Cys, Hcy, and GSH etc.) can undergo only mono-nucleophilic reaction. Therefore, probes **8-11** containing bis-electrophilic center were been developed for H₂S detection.³⁰⁻³² H₂S mediated nucleophilic addition reaction at aldehyde group forms a hemithioacetal intermediate which subsequently undergoes Michael addition to α , β -unsaturated ester/ketone on the aromatic ring. The resulting compound exhibited fluorescence enhancement because of blockage of PET process.

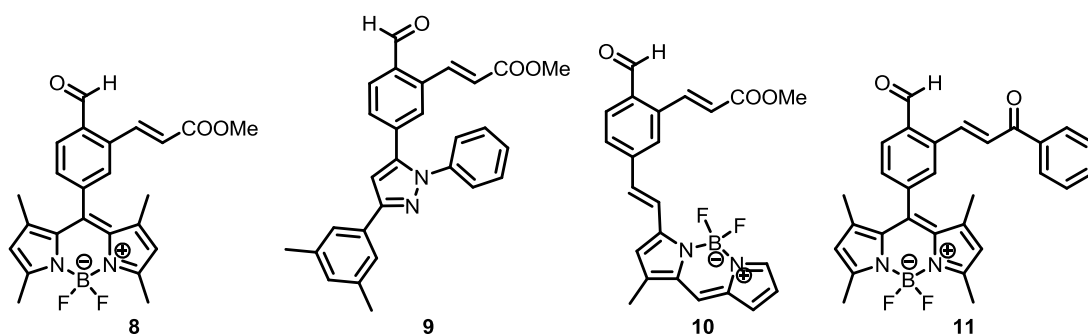


Figure 5. Structures of probes based on nucleophilic addition cyclization reactions by H₂S.

4) Thiolysis based probes: Thiol mediated removal of dinitrophenyle group in basic condition to deprotect tyrosine during the synthesis of peptide is well known in literature. Similarly, dinitrophenyl group can undergo thiolysis reaction in presence of H₂S (pK_a of H₂S ~7) at physiological pH. Removal of dinitrophenyl group from probes **12, 14-16**³³⁻³⁷ by H₂S mediated thiolysis reaction can change the fluorescence property of fluorophore.

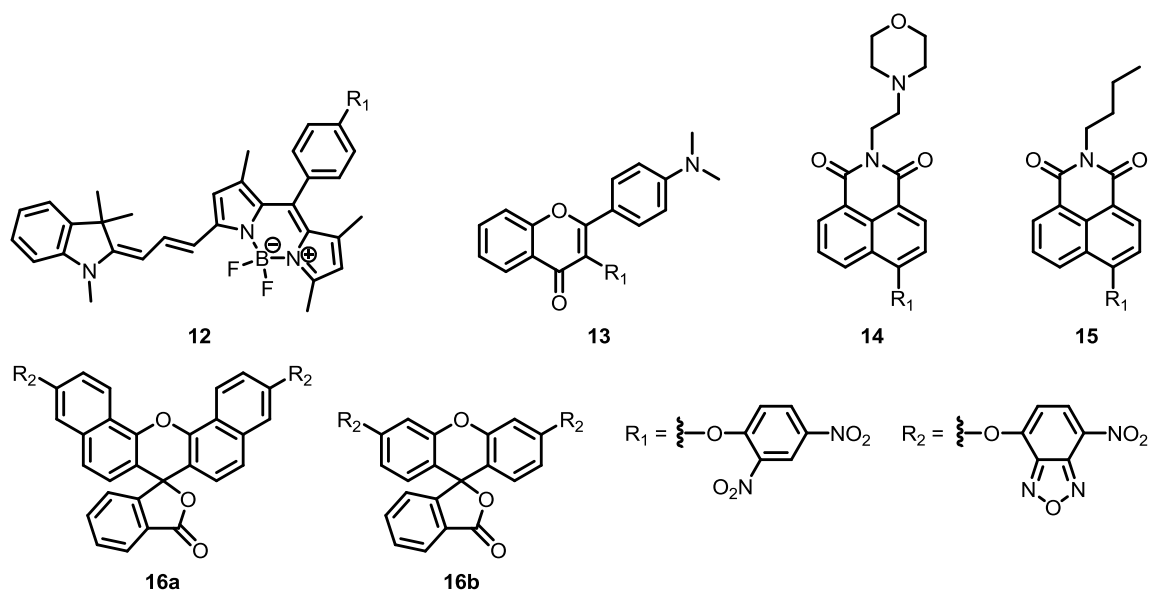


Figure 6. Structures of probes based on thiolysis by H₂S.

5) Azide to amine reduction: Azides can also be reduced to amine in presence of H₂S. Azide to amine reduction is relatively faster with H₂S compared to GSH and other biological thiols. Because of the difference in electronic behavior of azide and amine, H₂S mediated reduction of azide to amine was widely used to construct fluorescent probes for H₂S detection **21-27** (Figure 7)^{3,25,38-42}. Apart from involved PET and ICT pathways, azide can alter the fluorescent properties dramatically by altering the conjugation of the fluorophore. However, many of these probes suffer from drawback related to poor detection limit, and slow response time and incapability of detecting H₂S in endogenous and live cell.

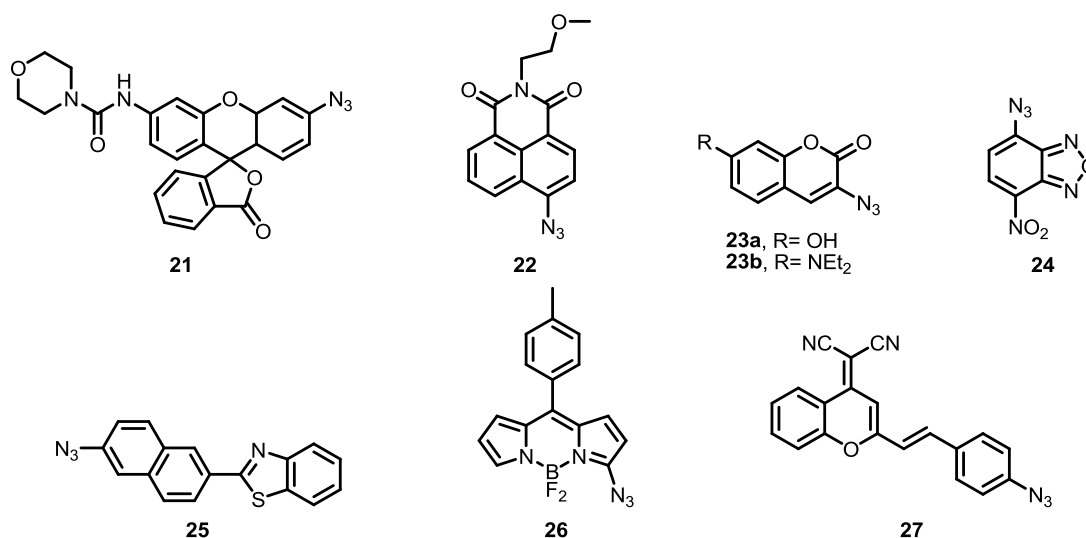


Figure 7. Structures of probes based on azide to amine reduction by H₂S.

6) **Cascade reaction based probe:** Cascade reaction based approach is expected to improve the reaction time of the sensing process because the enthalpically favorable process. Additionally, properties of these probes can also be tuned to infer better detection limit. For example, probes **28-31**⁴³⁻⁴⁶ are reported based on azide to amine reduction followed by cascade release of an immolative linker and the fluorophore. These probes have displayed sensitivity in the nanomolar concentration and ability to sense H₂S within living cells.

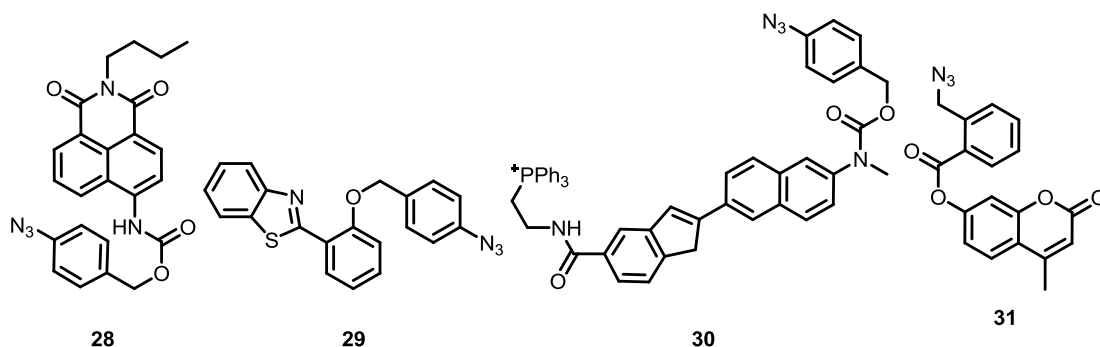


Figure 8. Structures of probes based on azide to amine reduction by H₂S followed by a cascade reaction.

Objective

Our aim was to construct a fluorescent probe for sensing of H₂S with better sensitivity, low detection limit and applicability in biological samples. H₂S mediated reduction of azide to amine and cascade reaction based probes came to our attention. The work described in the thesis addresses following two approaches:

a) The iminocoumarin **34** is reported as a fluorophore.⁴⁷ Therefore, the probe **32** was designed by connecting the (4-azidophenyl)methyl group to the fluorophore (Figure 9A). The H₂S mediated reduction of **32** to **33** was expected facilitate the formation of fluorophore **34**. The probe **32** was expected to be nonfluorescent and *off-on* response was envisaged based on the design.

b) Although there are several reports on various mechanisms of unmasking the fluorophore but our approach was discrete from previously existing fluorophore releasing mechanisms, here we have designed a probe which facilitates the synthesis of fluorophore in presence of H₂S. In this strategy, the linkage of the (4-azidophenyl)methyl group with 2-(4-(diethylamino)-2-hydroxybenzylidene)malononitrile was proposed to form the probe **36** (Figure 9B). The probe upon H₂S mediated reduction was expected to form the intermediate **37**. The intermediate **37** upon release of the immolative linker was expected to allow the Pinner cyclization⁴⁸ to release Iminocoumarin **38** and a byproduct **35**. A similar *off-on* response was proposed based on the design.

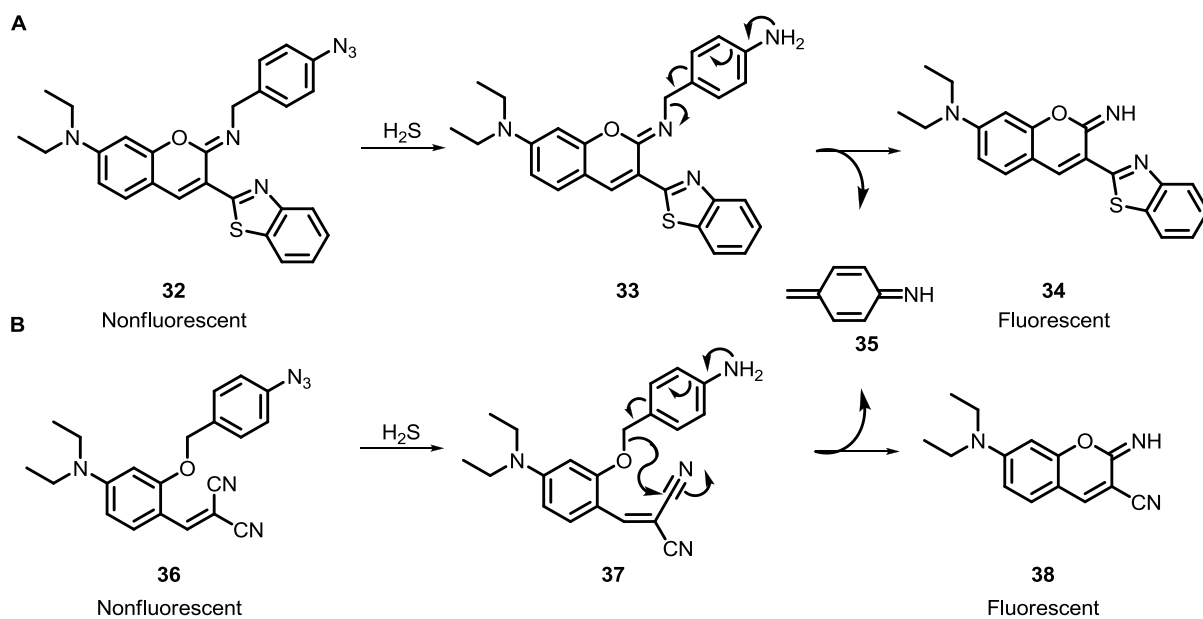


Figure 9. Strategies for the detection of H_2S , using an immolative linker **(A)** and formation of iminocoumarin using free hydroxy group **(B)**.

Materials and Methods

➤ General Methods:

All reactions were conducted under the nitrogen atmosphere. All the chemicals were purchased from commercial sources and used as received unless stated otherwise. Solvents: petroleum ether, ethyl acetate (EtOAc), dichloromethane (DCM), and methanol (MeOH) were distilled prior to thin layer and column chromatography. Column chromatography was performed on Merck silica gel (100–200 mesh). TLC was carried out with E. Merck silica gel 60-F-254 plates.

➤ Physical Measurements:

The ^1H and ^{13}C spectra were recorded on 400 MHz Jeol ECS-400 (or 100 MHz for ^{13}C) spectrometers using either residual solvent signals as an internal reference or from internal tetramethylsilane on the δ scale (DMSO- d_6 δH , 2.50 ppm, δC 39.52 ppm). The chemical shifts (δ) are reported in ppm and coupling constants (J) in Hz. The following abbreviations are used: m (multiplet), s (singlet), br s (broad singlet), d (doublet), t (triplet) dd (doublet of doublet), dt (doublet of triplet), q (quartet), and sex (sextet). High-resolution mass spectra were obtained from MicroMass ESI-TOF MS spectrometer. Absorption spectra were recorded on a Thermo Scientific, Evolution 300 UV-VIS spectrophotometer. Steady State fluorescence experiments were carried out in a micro fluorescence cuvette (Hellma, path length 1.0 cm) on a Horiba JobinYvon, FluoroMax-4 instrument. (FT-IR) spectra were obtained using Bruker: α ALPHA spectrophotometer (neat) and reported in cm^{-1} . Melting points were measured using a VEEGO Melting point apparatus. All melting points were measured in open glass capillary and values are uncorrected. Crystal structures were recorded on a Bruker single crystal X-Ray diffractometer. HPLC data was recorded using Agilent Eclips plus 5 μm column in gradient mode. Cell images were taken in 35 mm (diameter) dishes. The media (DMEM) and PBS buffer were purchased from commercial sources. Fluorescence images were taken using Olympus Inverted IX81 equipped with Hamamatsu Orca R2 microscope. ChemBio Draw Ultra and Image *J* software were used for drawing structure and for processing cell image respectively.

➤ Photophysical Measurements:

Preparation of the medium: Deionized water was used throughout all experiments. All experiments were carried out in water with 1% DMSO (maximum).

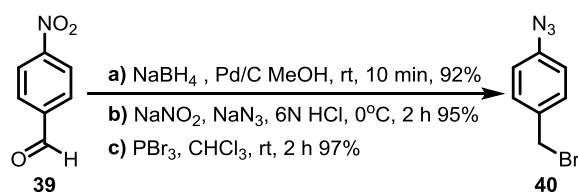
Preparation of the solution of probe and reporter: A stock solution of Probe (2000 μM) and Reporter (2000 μM) was prepared in DMSO. Final concentration of each of **35** and **36** during each assay was 10 μM with 1% DMSO (maximum).

Preparation of the solution of analyte: To prepare the stock solutions of Analytes appropriate amounts of Na_2S , cysteine (Cys), homocystein (Hcy), glutathione (GSH), NaF, NaCl, NaBr, NaI, $\text{Na}_2\text{S}_2\text{O}_3$, Na_2SO_3 , Na_2SO_4 , NaSCN, NaNO_2 , NaNO_3 , NaOH and H_2O_2 were dissolved separately in deionized water to provide stock solution of concentrations = 20 mM each. Calculated volume of an analyte was added from respective stock solutions to each fluorescence cuvette (2 mL) to provide final required analyte concentration. Calculated volume of analyt was added from stock solutions to each fluorescence cuvette (2 mL) to provide required final concentration. All spectral data were recorded at 30 min after the addition of analyte by exciting at respective absorption maxima of the fluorophore. The excitation and emission slit width were adjusted according to the activity of the fluorophore.

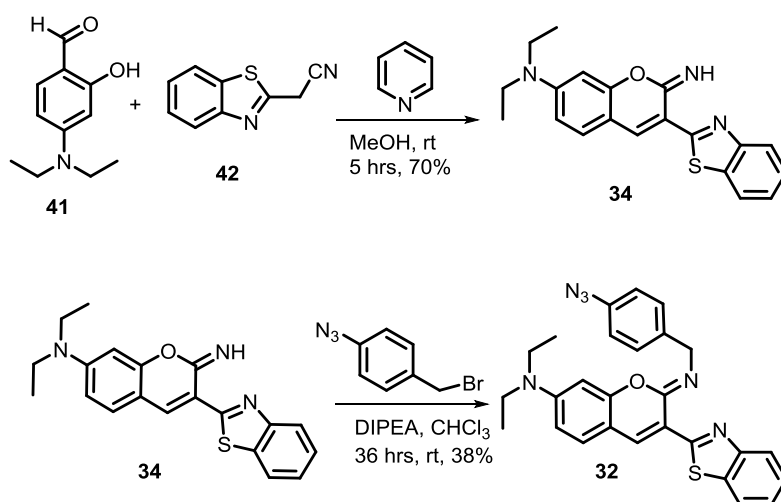
➤ Experimental Procedure:

Synthesis of Iminocoumarin Based probe:

Synthesis of immolative linker: Synthesis of immolative linker was carried out from 4-nitrobenzaldehyde using reported protocol and obtained data was matched with reported data.⁴⁹



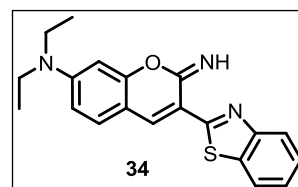
Scheme 1. Synthesis of immolative linker **40**.



Scheme 2. Synthesis of Iminocumarin based probe **32**.

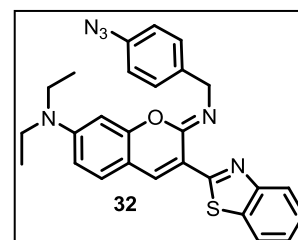
Synthesis of 3-(benzo[*d*]thiazol-2-yl)-*N,N*-diethyl-2-imino-2*H*-chromen-7-amine **34** (C₂₀H₁₉N₃OS):

To a solution of 2-benzothiazoleacetonitrile **42** (150 mg, 0.86 mmol) in 15 mL of dry methanol was added piperidine (850 μ L, 8.6 mmol) and the solution was stirred at room temperature for 3 min. Then 4-(diethylamino)salicylaldehyde **41** (166 mg, 0.86 mmol) was added. The mixture was stirred for 5 h at room temperature, and the precipitate was collected by filtration, washed with dry methanol, and dried under high vacuum to afford **34** (210 mg, 70%). **Melting point:** 192–193 °C; **¹H NMR** (400 MHz, DMSO-*d*₆) δ : 8.47 (s, 1H), 8.02 (d, *J* = 7.8 Hz, 1H), 7.91 (d, *J* = 7.8 Hz, 1H), 7.54 – 7.39 (m, 2H), 7.33 (d, *J* = 7.2 Hz, 1H), 6.57 (dd, *J* = 8.9, 2.4 Hz, 1H), 6.34 (s, 1H), 3.47 – 3.33 (m, 4H), 1.35 – 0.91 (m, 6H); **HRMS** (ESI): Calculated for C₂₀H₂₀N₃OS⁺[M+H]⁺: 350.1328, found: 350.1325. Data obtained was consistent with reported data⁴⁷.

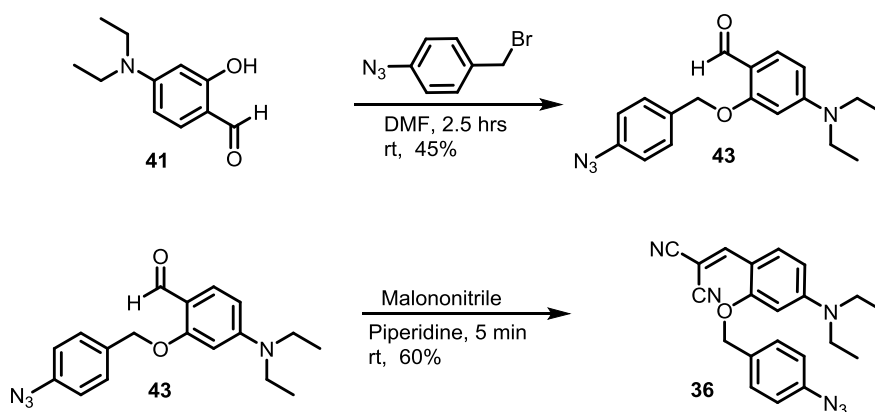


Synthesis of (*Z*)-2-(4-azidobenzylimino)-3-(benzo[*d*]thiazol-2-yl)-*N,N*-diethyl-2*H*-chromen-7-amine **32** (C₂₇H₂₄N₆OS):

To the solution of 3-(benzo[*d*]thiazol-2-yl)-*N,N*-diethyl-2-imino-2*H*-chromen-7-amine **34** (200 mg, 0.572 mmol) in 5 mL of dry chloroform was added di-isopropylethyleamine (DIPEA) (136 μ L, 0.686 mmol) and then 1-azido-4-(bromomethyl)benzene **40** (121.3 mg, 0.572 mmol) was added. The mixture was stirred for 36 h at room temperature, after completion of the reaction; the reaction mixture was extracted with Ethyl acetate (20 mL \times 3). The combined organic layer was washed with water (10 mL \times 3), brine (30



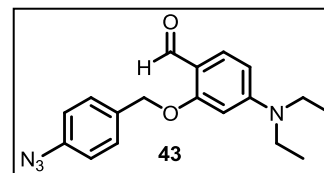
mL) and dried over Na₂SO₄. The solvent was removed under reduced pressure to obtain a yellow residue which was purified by column chromatography over silica gel (Eluent: 6 % EtOAc in petroleum ether) to furnish the pure **26** (107 mg, 38%) as yellow solid. **Melting Point:** 192–193 °C **IR** (KBr): ν/cm^{-1} 3740, 3226, 2862, 2110, 1640, 1517, 1517, 1119, 1073; **¹H NMR** (400 MHz, DMSO-d₆) δ 8.58 (s, 1H), 8.06 (d, *J* = 7.9 Hz, 1H), 7.96 (d, *J* = 8.1 Hz, 1H), 7.64 (d, *J* = 8.4 Hz, 2H), 7.57 (d, *J* = 8.8 Hz, 1H), 7.52 – 7.43 (m, 1H), 7.41 – 7.31 (m, 1H), 7.14 (d, *J* = 8.5 Hz, 2H), 6.63 (dd, *J* = 8.9, 2.3 Hz, 1H), 6.54 (d, *J* = 2.1 Hz, 1H), 4.84 (s, 2H), 3.45 (q, *J* = 6.9 Hz, 4H), 1.14 (t, *J* = 7.0 Hz, 6H); **¹³C NMR** (100 MHz, DMSO-D₆) δ 161.3, 155.2, 151.7, 151.0, 148.3, 137.7, 137.2, 136.2, 134.4, 130.2, 128.9, 125.5, 123.8, 121.5, 121.1, 118.6, 115.2, 108.4, 107.3, 96.3, 48.8, 43.8, 12.1. **HRMS** (ESI): Calculated for C₂₇H₂₅N₆O⁺[M+H]⁺: 481.181; found: 481.1809.



Scheme 3. Synthesis of Iminocumarin based Probe.

Synthesis of 2-(4-azidobenzoyloxy)-4-(diethylamino)benzaldehyde **43**

(C₁₈H₂₀N₄O₂): In a 25 mL round bottom flask 1-azido-4-(bromomethyl)benzene (200 mg, 1.34 mmol) was dissolved in 5 mL DMF; 4-(diethylamino)-2-hydroxybenzaldehyde **41** (258mg, 1.34 mmol) and K₂CO₃ (277.8mg, 2.01 mmol) was

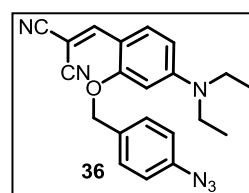


added. The reaction mixture was stirred at room temperature for 2.5 h. After completion of the reaction, the reaction mixture was extracted with Ethyl acetate (20 mL × 3). The combined organic layer was washed with water (10 mL × 3), brine (30 mL) and dried over Na₂SO₄. The solvent was removed under reduced pressure to obtain a brown residue which was purified by column chromatography over silica gel

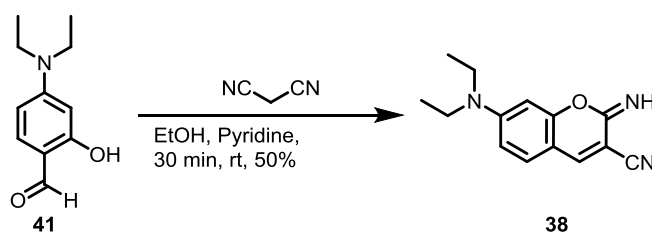
(Eluent: 10 % EtOAc in petroleum ether) to furnish the pure **43** (215 mg, 50%) as colourless liquid. **IR** (KBr): ν/cm^{-1} 3326, 3210, 2975, 2129, 1728, 1613, 1556, 1513, 1120, 1075; **$^1\text{H NMR}$** (400 MHz, DMSO- d_6): δ 10.06 (s, 1H), 7.53 (d, $J = 8.5$ Hz, 2H), 7.52 (d, $J = 9$ Hz, 1H), 7.13 (d,t $J = 8.2, 2.2$ Hz, 2H), 6.33 (dd, $J = 8.9, 1.9$ Hz, 1H), 6.21 (d, $J = 2.2$ Hz, 1H), 5.24 (s, 2H), 3.40 (q, $J = 7.0$ Hz, 4H), 1.08 (t, $J = 7.0$ Hz, 6H); **$^{13}\text{C NMR}$** (100 MHz, DMSO- D_6): δ 185.7, 163.0, 154.0, 139.4, 134.3, 130.1, 129.7, 119.7, 113.9, 104.9, 94.8, 69.2, 44.6, 12.9; **HRMS** (ESI): Calculated for $\text{C}_{18}\text{H}_{21}\text{N}_4\text{O}_2^+[\text{M}+\text{H}]^+$: 325.1644; found: 325.1664.

Synthesis of 2-(2-(4-azidobenzoyloxy)-4-

(diethylamino)benzylidene)malononitrile **36** ($\text{C}_{21}\text{H}_{20}\text{N}_6\text{O}$): In a 25 mL round bottomed flask 2-(4-azidobenzoyloxy)-4-(diethylamino)benzaldehyde **43** (190 mg, 0.58 mmol), malononitrile (38.7 mg, 0.58 mmol) and piperidine (248 mg, 2.9



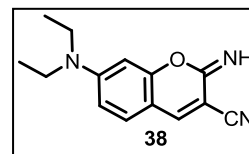
mmol) were dissolved in ethanol (5 mL). The reaction mixture was stirred at room temperature for 5 min. The yellow residue obtained after evaporation of ethanol under reduced pressure, was purified by column chromatography over silica gel (Eluent: 20 % EtOAc in petroleum ether) to furnish the pure **36** (130 mg, 60%) as a yellow solid. **Melting Point:** 139-141 °C. **IR** (KBr): ν/cm^{-1} 3327, 3210, 2975, 2217, 2131, 1613, 1557, 1514, 1118, 1075; **$^1\text{H NMR}$** (400 MHz, DMSO- D_6): δ 8.03 (d, $J = 9.3$ Hz, 1H), 7.92 (s, 1H), 7.53 (d, $J = 8.3$ Hz, 2H), 7.15 (d, $J = 8.3$ Hz, 2H), 6.54 (dd, $J = 9.3, 1.2$ Hz, 1H), 6.23 (d, $J = 1.3$ Hz, 1H), 5.25 (s, 2H), 3.48 (q, $J = 6.8$ Hz, 4H), 1.09 (t, $J = 6.9$ Hz, 6H); **$^{13}\text{C NMR}$** (100 MHz, DMSO- D_6): δ 161.0, 155.0, 150.6, 139.7, 133.7, 130.4, 130.1, 119.8, 117.6, 116.6, 109.2, 106.8, 94.7, 69.7, 66.2, 45.0, 13.0; **HRMS** (ESI) Calculated for $\text{C}_{21}\text{H}_{21}\text{N}_6\text{O}^+[\text{M}+\text{H}]^+$: 373.1777; found: 373.1772.



Scheme 4. Synthesis of Iminocoumarin **38**.

Synthesis of 7-(diethylamino)-2-imino-2H-chromene-3-carbonitrile 38

(C₁₄H₁₅N₃O): In a 25 mL round bottom flask 4-(diethylamino)-2-hydroxybenzaldehyde **41** (100 mg, 0.52 mmol) and Malononitrile (34.36 mg, 0.52 mmol) were added in ethanol (5 mL) with a drop



of piperidine. Reaction mixture was stirred for 30 min at room temperature. After completion of the reaction, the reaction mixture was evaporated under reduced pressure to remove EtOH, obtained a yellow residue which was purified by column chromatography over neutral alumina (Eluent: 2 % EtOAc in petroleum ether) to furnish the pure **38** (62 mg, 50%) as yellow solid. Obtained data was consistent with the literature data.⁴⁸

Results and discussion

Photophysical studies of Coumarin based Probe 32.

To formalize *off-on* nature of probe **32** all photophysical measurements were done in water. The absorption spectrum of probe **32** was found at $\lambda_{\text{max}} = 485$ nm and very low fluorescence intensity was observed upon exciting at same wavelength. On the other hand under undifferentiated condition iminocoumarin **34** gives absorption spectrum at $\lambda_{\text{max}} = 485$ nm, fluorescence spectra recorded at $\lambda_{\text{ex}} = 485$ nm for iminocoumarin **34** gives strong emission at $\lambda_{\text{max}} = 524$ nm. From the data describes above we can formulate that Probe **32** can act as a turn on fluorescence probe for the detection of Na_2S .

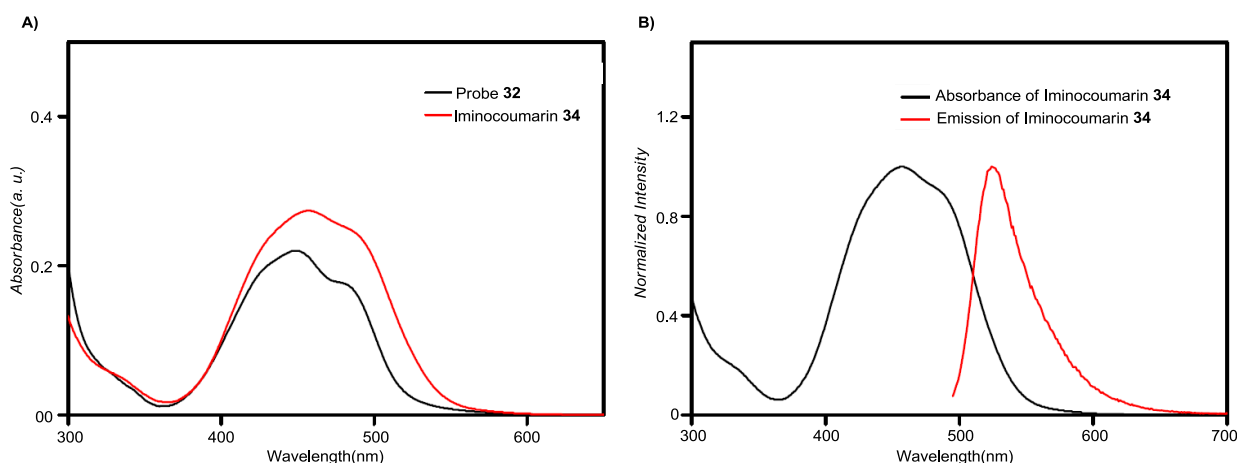


Figure 10. (A) Absorption spectrum of Probe **32** (10 μM) and iminocoumarin **34** (10 μM) in water **(B)** Normalized absorption and Emission spectrum of iminocoumarin **34**.

To check the sensing ability of Probe **32** towards H_2S , fluorescence spectra were recorded before and after addition of 100 eq. Na_2S . No significant change in fluorescence intensity was observed even after 30 mint of addition of Na_2S . Hence, in spite of having distinguishable photophysical properties probe **32** cannot act as a sensor for H_2S .

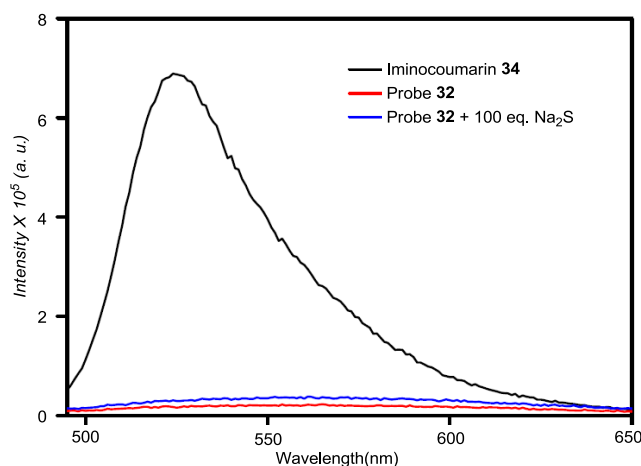


Figure 11. Emission spectrum of Probe **32** (10 μM) after 30 minutes of addition of 100 eq. of Na_2S and Iminocoumarin **34** in water when excited at $\lambda_{\text{ex}} = 485 \text{ nm}$.

Therefore, the probe **32** was synthesized successfully but failed to fulfill the purpose of sensing H_2S . Probe **32** did not show significant enhancement in fluorescence when treated with Na_2S . In next stage we have modified our strategy to construct a fluorophore during the sensing mechanism. The new probe **36** contains a self immolative linker which got cleaved by H_2S mediated reduction of azide to amine resulting Pinner cyclization to form a iminocoumarine derivative with a simultaneous enhancement of fluorescence.

Photophysical studies of Iminocoumarin based Probe **36**.

To investigate the *off-on* nature of probe **36** and iminocoumarin **38** all photophysical properties were recorded in water-EtOH (9:1) with 1 mM CTAB (Cetyltrimethylammonium bromide). The absorption spectrum of probe **36** exhibited at $\lambda_{\text{max}} = 450 \text{ nm}$ (Figure 12A) with molar extinction coefficient, $\epsilon = 30020 \text{ M}^{-1} \text{ cm}^{-1}$. A very faint red emission at $\lambda_{\text{max}} = 575 \text{ nm}$ was observed when fluorescence property of probe **36** (10 μM) was recorded under identical condition $\lambda_{\text{ex}} = 440 \text{ nm}$.

On the other hand, Iminocoumarine **38** gives absorption spectrum at $\lambda_{\text{max}} = 438 \text{ nm}$ with molar extinction coefficient $\epsilon = 36150 \text{ M}^{-1} \text{ cm}^{-1}$ under undifferentiated condition. A strong fluorescence intensity (at $\lambda_{\text{em}} = 480 \text{ nm}$) of iminocoumarin **38** was observed upon exciting at $\lambda_{\text{ex}} = 440 \text{ nm}$ in water-EtOH (9:1) with 1 mM CTAB (Figure

12). Above data satisfies the criteria of probe **36** to be an efficient ratiometric chemodosimeter for H₂S.

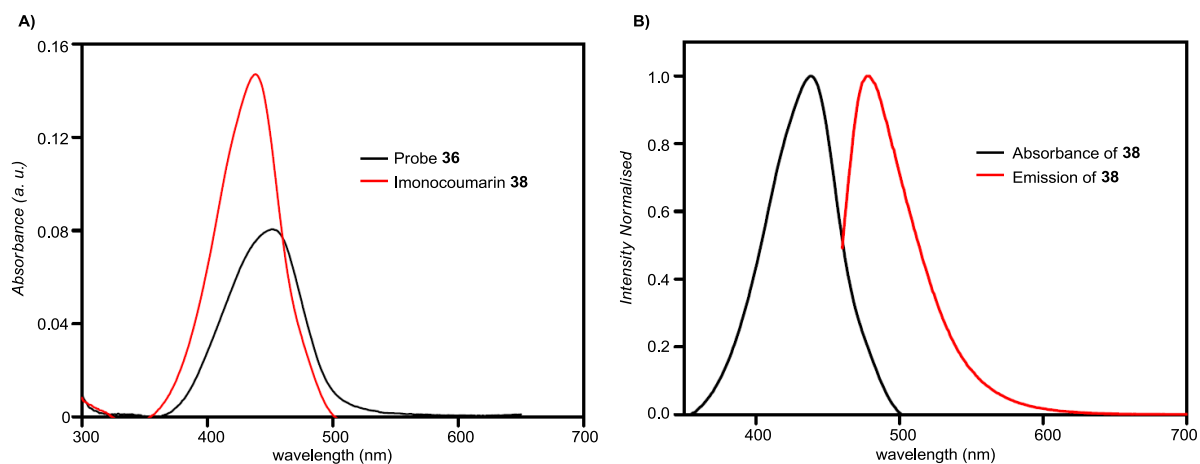


Figure 12. **A)** Absorption spectrum of probe **36** (10 μ M) and iminocoumarin **38** in water-EtOH (9:1) with 1 mM CTAB. **B)** Normalized absorption and Emission spectrum of iminocoumarin **38**.

In next stage sensing ability of probe **36** was evaluated by recording fluorescence spectra before and after addition of Na₂S (15 eq.). A sharp enhancement in fluorescence intensity at $\lambda_{em} = 480$ nm with a shifting of emission maxima was observed (Figure 13) after 30 mint of addition of Na₂S to probe **36** (in water-EtOH (9:1) with 1 mM CTAB). This data signifies that Probe **36** can be a reliable candidate to detect H₂S.

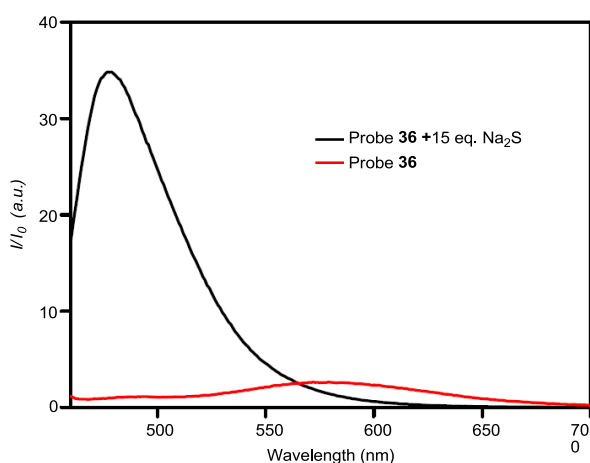


Figure 13. Emission spectrum of probe **36** before and after addition of 15 eq. of Na₂S in water-EtOH (9:1) with 1 mM CTAB. Spectra was recorded after 30 minutes of addition of Na₂S, $\lambda_{ex} = 440$ nm.

Response time of probe **36** towards H₂S detection was evaluated by recording fluorescence spectra with time. Probe **36** (10 μM) was treated with Na₂S (150 μM) in water-EtOH (9:1) 1mM CTAB, and change in fluorescence intensity was recorded with time at $\lambda_{em} = 480$. When the fluorescence intensity at definite time interval (at $\lambda_{em} = 480$ nm) was plotted against time, a pseudo first order reaction kinetics was observed with rate constant $k = 0.11294 \text{ min}^{-1}$ and half life $t_{1/2} = 6.136 \text{ min}$ (Appendix Figure 20). On the other hand, when the fluorescence intensity of probe **36** was monitored without any analyte in water-EtOH (9:1) 1mM CTAB, no significant enhancement in fluorescence intensity was observed even after 30 mint, which indicates the stability of probe **36** in the solvent medium (Figure 14). In addition to that, the inertness of probe **36** was established by recording kinetics profile in presence of various biothiols (Cys, Hcy and GSH). No enhancement in fluorescent intensity signifies the applicability of probe **36** in biological systems because of inertness towards the competitive biothiols.

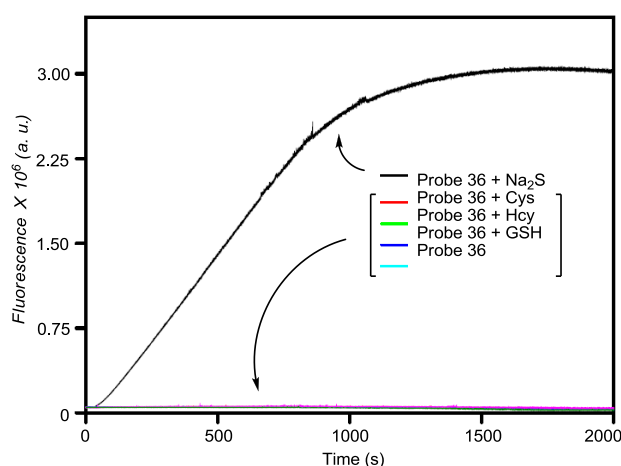


Figure 14. Change in fluorescence intensity of probe **36** (10 μM) with time (at $\lambda_{em} = 480$ nm) upon addition of Na₂S, Cys, Hcy and GSH (150 μM each) in water-EtOH (9:1) 1mM CTAB.

The sensitivity of probe **36** towards H₂S prompted us to evaluate the selectivity of probe in an isolated and competitive environment with other biorelevant species. Probe **36** (10 μM) was treated with 150 μM (15 Equiv.) of each specie (F⁻, Cl⁻, Br⁻, I⁻, NO₂⁻, NO₃⁻, S₂O₃²⁻, SO₃²⁻, SO₄²⁻, SCN⁻, Cys, Hcy, GSH, NaOH, H₂O₂) separately for 30 mint and fluorescence spectra were recorded in water-EtOH (9:1) 1mM CTAB at $\lambda_{ex} = 440$. Negligible emission intensity was observed for all analytes

(Figure 15, front row). Then Na₂S (150 μM) was added to the same solution of different analytes, a sharp rise in emission intensity was observed in individual competing analyte which are comparable with the fluorescence rise in case of only Na₂S (Figure 15, back row). .

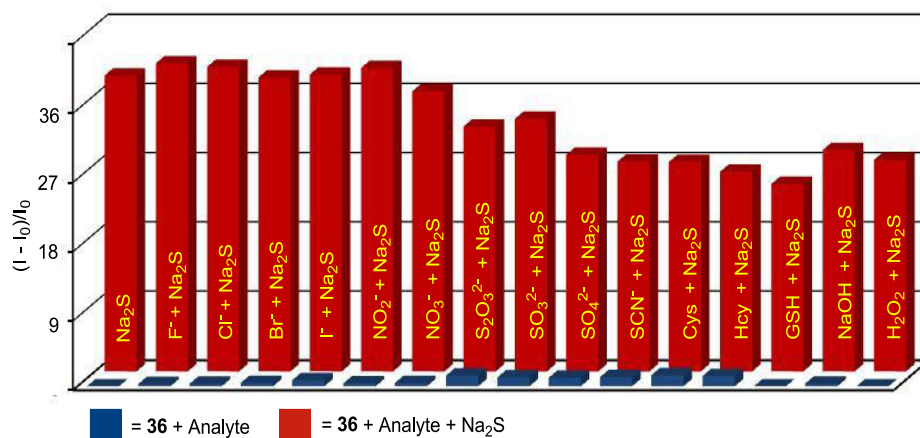


Figure 15. Relative fluorescence intensity enhancements [(I-I₀)/I₀] at 480 nm for probe **36** (10 μM) towards Na₂S (150 μM) in water-EtOH (9:1) 1mM CTAB. Front row: change in intensities in the presence of various analytes (150 μM); back row: Na₂S was added in the presence of respective analyte.

Quantitative response of probe **36** towards H₂S was evaluated by fluoremetric titration. Emission spectra of probe **36** were recorded (in water-EtOH (9:1) 1mM CTAB, at λ_{ex} = 440 nm) with increasing concentration of Na₂S. A stepwise enhancement in fluorescence intensity at λ_{em} = 480 nm was observed (Figure 16). When fluorescence intensity at 480 nm was plotted against concentration of Na₂S added, an excellent linear correlation was observed (regression factor, R² = 0.9947) upto 5 equivalent of Na₂S (Figure 16, *inset*).

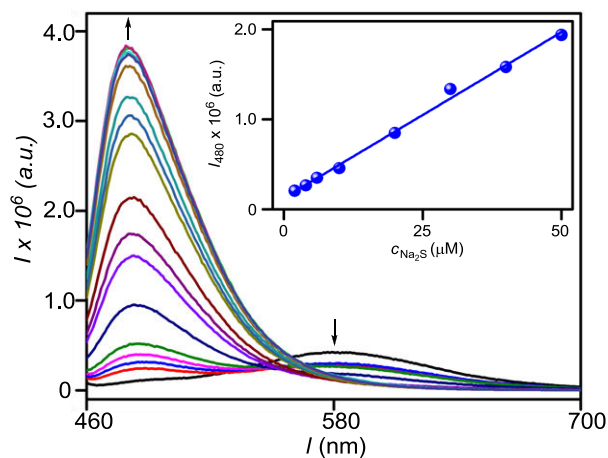


Figure 16. Fluorescence spectral changes of probe **36** (10 μM) upon addition of different concentrations of Na_2S in water/EtOH (9:1) 1 mM CTAB). *Inset:* Linear relationship between fluorescence intensity at 480 nm versus concentration of Na_2S added in water-EtOH (9:1) 1mM CTAB.

Determination of the Limit Of Detection (LOD) of probe 36:

The Limit Of Detection (LOD) of 169 nM was calculated (Table 1) for probe **36**, upon sensing of H_2S , by using Eq. 1.

$$LOD = 3\sigma/m \quad \text{Eq. 1}$$

where, σ = standard deviation of 8 blank measurements (*i.e.* fluorescence intensity of only probe **36** at $\lambda_{em} = 480$ nm), m = slope of the concentration profile obtained from Intensity of fluorescence enhancement plotted with respect to concentration (Figure Appendix 21). The signal-to-noise ratio S/N for the measurement was considered as 3:1.

Table 1. Calculation of the limit of detection (*LOD*) of H₂S sensing:

| S. No. | <i>I</i> ₄₈₀ of 36 | σ | <i>m</i> | $3\sigma/m$ |
|--------|--------------------------------------|-------------|-----------------------------|---------------------------|
| 1 | 90501.09 | 2289.302106 | 40595.62 μM^{-1} | 0.169178503 μM |
| 2 | 92586.99 | | | or |
| 3 | 91854.08 | | | 169.178503 nM |
| 4 | 88023.81 | | | |
| 5 | 94085.16 | | | |
| 6 | 93412.03 | | | |
| 7 | 94977.22 | | | |
| 8 | 90247.79 | | | |

Determination of quantum yields for 36 and 38: The quantum yield of probe **36** and Iminoumarin **38** were determined according to the following Eq. 2:

$$\Phi_1 = \Phi_B \times \frac{I_1 \times A_B \times \lambda_{exB} \times (\eta_1)^2}{I_B \times A_1 \times \lambda_{ex1} \times (\eta_B)^2} \quad \text{Eq. 2}$$

where, Φ is quantum yield; *I* is integrated area under the emission spectra; *A* is absorbance at the excitation wavelength; λ_{ex} is the excitation wavelength; η is the refractive index of the solution; the subscripts **1** and **B** refer to the unknown and the standard, respectively. Coumarin-153 was used as standard in 50% ethanol-water ($\Phi = 0.032$) for probe **36** and same standard was used in acetonitrile ($\Phi = 0.56$) for iminocoumarin **38**.

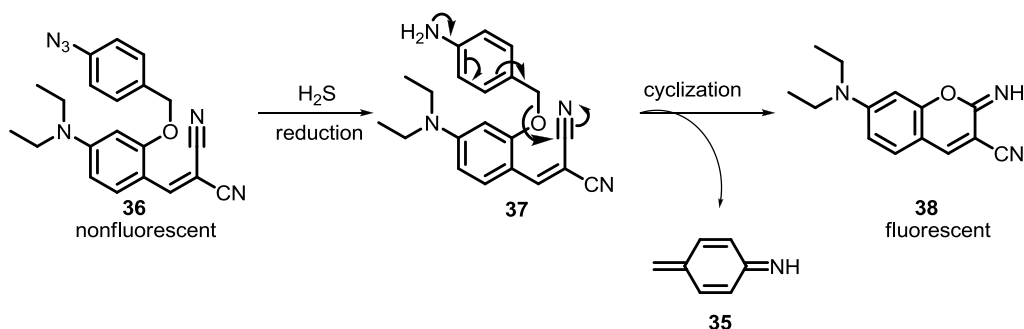
The quantum yield (Φ) values are 0.05750 and 0.00134 for probe **36** and iminocoumarin **38** respectively. A 43 fold difference of quantum yield was observed for iminocoumarin **38** to probe **36**.

Table 2. Comparison of Quantum yield values for probe **36** and **38**.

| Compound | λ_{max} (nm) | ϵ ($\text{M}^{-1} \text{cm}^{-1}$) | λ_{em} (nm) ^a | Φ |
|-----------|----------------------|---|----------------------------------|---------|
| 35 | 450 | 30020 | 580 | 0.00134 |
| 36 | 438 | 36150 | 480 | 0.05750 |

^a $\lambda_{ex} = 440$ nm.

Sensing mechanism of Cascade Probe 36:



Scheme 5. H_2S sensing mechanism of ratiometric probe **36**.

For the validation of proposed sensing mechanism of probe **36** and confirmation of the formation Iminocoumarin **38** as reporter molecule during the course of reaction with H_2S , HPLC titration was performed. Chromatograms were recorded in gradient method using acetonitrile and water as eluent. Using undifferentiated conditions, probe **36** and iminocoumarin **38** exhibited retention time, $t_R = 9.16$ and 4.99 min, respectively (Fig. 17). When HPLC chromatogram of reaction mixtures containing probe **36** and increased concentrations of Na_2S (5 and 10 equiv in water-EtOH (9:1) 1mM CTAB) were recorded, peak corresponding to probe **36** started decreasing (at $t_R = 9.16$) with a simultaneous enhancement of the peak (at $t_R = 4.99$) corresponding to iminocoumarin **38** was observed. This data confirms the reaction of probe **36** with H_2S results the formation of iminocoumarin **38** as a fluorescent reporter molecule.

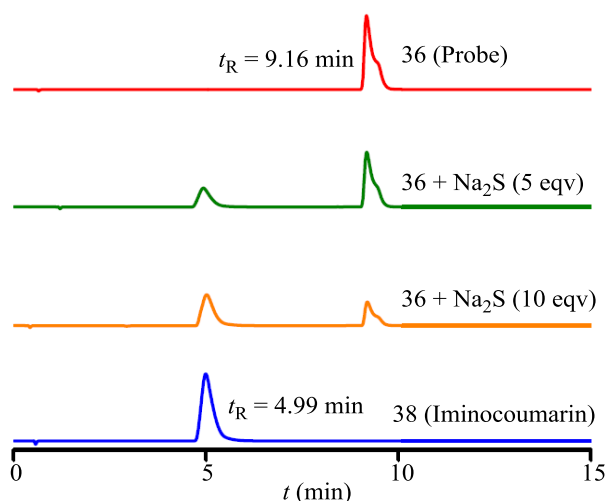


Figure 17. HPLC chromatograms of Probe **36** (100 μ M) on titration with Na_2S (5 and 10eq.) recorded in solvent system of acetonitrile and water. HPLC chromatograms of pure probe **36** (100 μ M, red line) and iminocoumarin **38** (100 μ M, blue line) are also shown.

For further investigation of proposed mechanism a small scale reaction of probe **36** was carried out with Na_2S (2 Eqv.) in EtOH for 5 min, and the mixture was analyzed by mass spectrometry. Signals corresponding to both **36** ($m/z = 395.2487$ for $[\mathbf{36}+\text{Na}^+]$) and iminocoumarin **38** ($m/z = 264.1599$ for $[\mathbf{38}+\text{Na}^+]$) were observed (Figure 18).

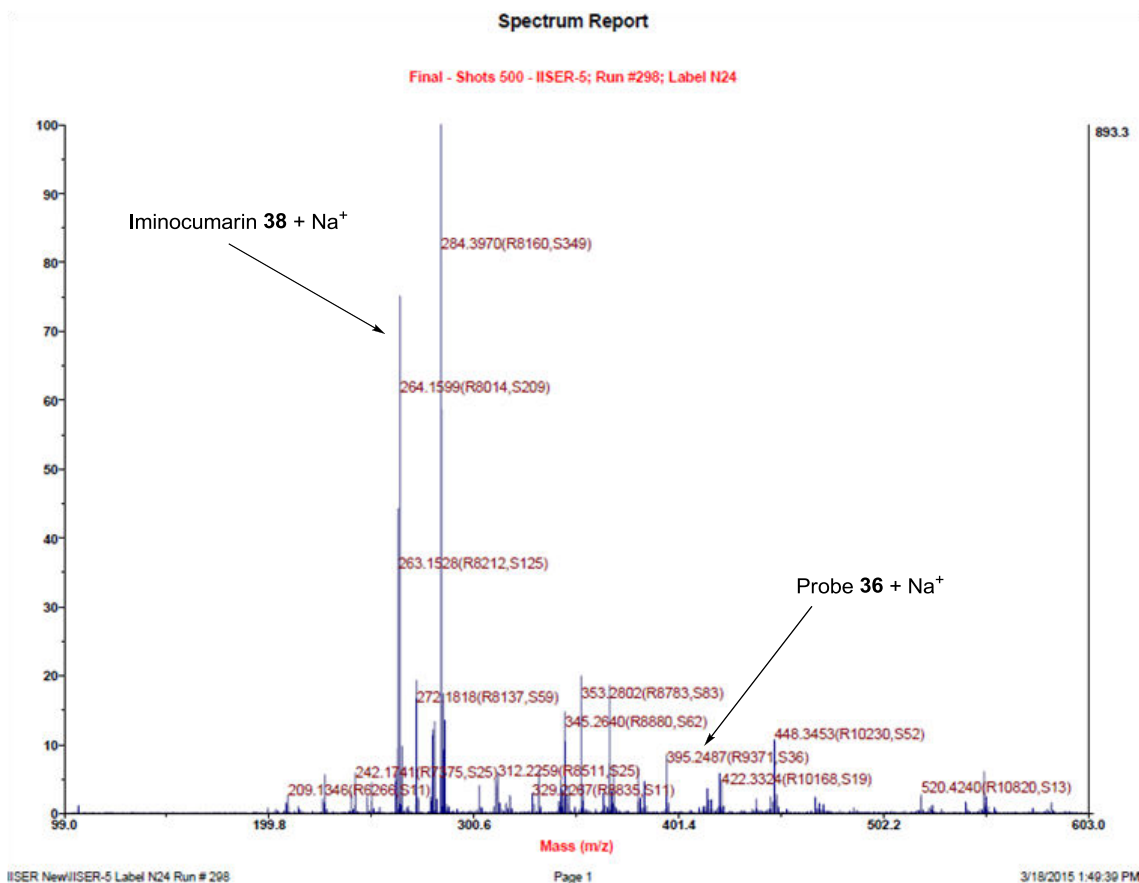


Figure 18. Mass spectrometry (MALDI) data of the reaction mixture containing probe **36** and Na₂S.

Cell permeability and capability of the probe **36** to selectively detect intracellular H₂S was evaluated by live-cell imaging studies. Human cervical cancer cell-line (HeLa) was used for cell imaging studies. A weak fluorescence intensity was observed when HeLa cells were incubated with only probe **36** (10 μM in 1:100 DMSO-DMEM v/v, pH = 7.4) at 37 °C for 30 min (Figure 19B). Then the same HeLa cells (pre-incubated with probe **36**) were incubated with Na₂S (100 μM in 1:100 H₂O-DMEM, pH=7.4) at 37 °C for 30 min, strong fluorescence inside the cell were observed (Figure 19E). Appearance of faint fluorescence upon treating HeLa cells with probe **36** (Figure 19B) confirms its reaction with intracellular H₂S already present in these cells.

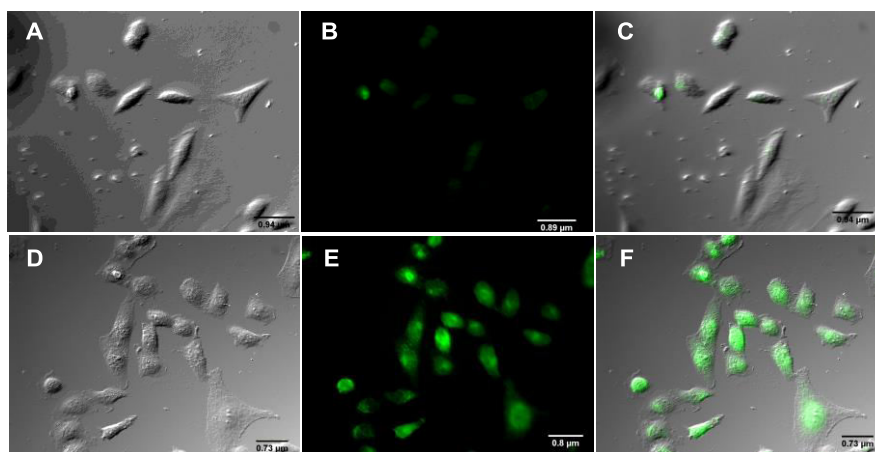


Figure 19. Image of HeLa cells: brightfield (A), fluorescence (B), and overlay (C), incubated with probe **36** (10 μ M) for 30 min. (D-F) are the respective brightfield, fluorescence and overlay image of HeLa cells pre incubated with probe **36** followed by Na₂S (100 μ M) incubation for 30 min.

In case of cascade based fluorescent probes **28-31** were reported. Probe **29** gives good fold enhancement but response time was quite high, in case of Probe **28** response time was improved but fold enhancement was compromised and probe **31** was not good in case of detection limit, probe **30** gives good ratiometric detection but again failed in response time and our new probe **36** provides a better limit of detection in optimum response time with better fold enhancement in fluorescence.

Table 3. Comparison of reported probes 28-31⁽⁴³⁻⁴⁶⁾ with probe 36.

| Probe | λ_{ex} nm | Response Time | Limit of detection | Fold enhancement |
|-----------|--------------------------|---------------|--------------------|------------------|
| 28 | 474 | 20 min | 110 nM | 24 |
| 29 | 465 | 60 min | 240 nM | 43 |
| 30 | 545 | 90 min | 200 nM | 09 |
| 31 | 450 | 20-40 min | 10 μ M | N/A |
| 36 | 480 | 25 min | 169 nM | 31 |

Conclusion

In summary we have synthesised a ratiometric probe for rapid and selective detection of H₂S with low detection limit and better fold enhancement.. The probe is capable to detect H₂S in presence of biological thiols (Cys, Hcy, GSH), ROS, reducing agents and other biological nucleophiles with response time of 25 min. and low detection limits (169 nM in water-EtOH(9:1) 1 mM CTAB) and cell permeability of probe **36** shows the importance in resolution of the alteration in concentrations of H₂S in mammalian cells.

References

- (1) Yu, F.; Han, X.; Chen, L. *Chem. Commun.* **2014**, *50*, 12234.
- (2) Goldman, E. R.; Medintz, I. L.; Whitley, J. L.; Hayhurst, A.; Clapp, A. R.; Uyeda, H. T.; Deschamps, J. R.; Lassman, M. E.; Mattoussi, H. *J. Am. Chem. Soc.* **2005**, *127*, 6744.
- (3) Lippert, A. R.; New, E. J.; Chang, C. J. *J. Am. Chem. Soc.* **2011**, *133*, 10078.
- (4) Dunn, K. W.; Mayor, S.; Myers, J. N.; Maxfield, F. R. *FASEB J.* **1994**, *8*, 573.
- (5) Zhang, J.-H.; Chung, T. D. Y.; Oldenburg, K. R. *J. Biomol. Screen.* **1999**, *4*, 67.
- (6) Singh, S.; Padovani, D.; Leslie, R. A.; Chiku, T.; Banerjee, R. *J. Biol. Chem.* **2009**, *284*, 22457.
- (7) Boehning, D.; Snyder, S. H. *Annu. Rev. Neur.* **2003**, *26*, 105.
- (8) Shibuya, N.; Tanaka, M.; Yoshida, M.; Ogasawara, Y.; Togawa, T.; Ishii, K.; Kimura, H. *Antioxid. Redox Sign.* **2008**, *11*, 703.
- (9) Li, L.; Rose, P.; Moore, P. K. *Annu. Rev. Pharma. Toxicol.* **2011**, *51*, 169.
- (10) Li, Q.; Lancaster Jr, J. R. *Nitric Oxide* **2013**, *35*, 21.
- (11) Lefer, D. J. *Br. J. Pharmacol.* **2008**, *155*, 617.
- (12) Baskar, R.; Bian, J. *Eur. J. Pharmacol.* **2011**, *656*, 5.
- (13) Kabil, O.; Motl, N.; Banerjee, R. *Biochim. Biophys. Acta, Proteins Proteomics* **2014**, *1844*, 1355.
- (14) Peng, Y.-J.; Nanduri, J.; Raghuraman, G.; Souvannakitti, D.; Gadalla, M. M.; Kumar, G. K.; Snyder, S. H.; Prabhakar, N. R. *Proc. Nat. Acad. Sci.* **2010**, *107*, 10719.
- (15) Yang, G.; Wu, L.; Wang, R. *FASEB J.* **2006**, *20*, 553.
- (16) Wallace, J. L. *Trends Pharmacol. Sci.* **2007**, *28*, 501.
- (17) Fiorucci, S.; Antonelli, E.; Mencarelli, A.; Orlandi, S.; Renga, B.; Rizzo, G.; Distrutti, E.; Shah, V.; Morelli, A. *Hepatology* **2005**, *42*, 539.
- (18) Yang, W.; Yang, G.; Jia, X.; Wu, L.; Wang, R. *J. Physiol.* **2005**, *569*, 519.
- (19) Eto, K.; Asada, T.; Arima, K.; Makifuchi, T.; Kimura, H. *Biochem. Biophys. Res. Commun.* **2002**, *293*, 1485.

- (20) Kamoun, P.; Belardinelli, M.-C.; Chabli, A.; Lallouchi, K.; Chadefaux-Vekemans, B. *Am. J. Med. Genet. Part A* **2003**, *116A*, 310.
- (21) Hannestad, U.; Margheri, S.; Sörbo, B. *Anal. Biochem.* **1989**, *178*, 394.
- (22) Lawrence, N. S.; Deo, R. P.; Wang, J. *Anal. Chim. Acta* **2004**, *517*, 131.
- (23) Siegel, L. M. *Anal. Biochem.* **1965**, *11*, 126.
- (24) Wang, R.; Yu, F.; Chen, L.; Chen, H.; Wang, L.; Zhang, W. *Chem. Commun.* **2012**, *48*, 11757.
- (25) Montoya, L. A.; Pluth, M. D. *Chem. Commun.* **2012**, *48*, 4767.
- (26) Wu, M.-Y.; Li, K.; Hou, J.-T.; Huang, Z.; Yu, X.-Q. *Org. Biomol. Chem.* **2012**, *10*, 8342.
- (27) Xuan, W.; Pan, R.; Cao, Y.; Liu, K.; Wang, W. *Chem. Commun.* **2012**, *48*, 10669.
- (28) Wang, B.; Li, P.; Yu, F.; Song, P.; Sun, X.; Yang, S.; Lou, Z.; Han, K. *Chem. Commun.* **2013**, *49*, 1014.
- (29) Lou, Z.; Li, P.; Pan, Q.; Han, K. *Chem. Commun.* **2013**, *49*, 2445.
- (30) Qian, Y.; Karpus, J.; Kabil, O.; Zhang, S.-Y.; Zhu, H.-L.; Banerjee, R.; Zhao, J.; He, C. *Nat. Commun.* **2011**, *2*, 495.
- (31) Li, X.; Zhang, S.; Cao, J.; Xie, N.; Liu, T.; Yang, B.; He, Q.; Hu, Y. *Chem. Commun.* **2013**, *49*, 8656.
- (32) Qian, Y.; Zhang, L.; Ding, S.; Deng, X.; He, C.; Zheng, X. E.; Zhu, H.-L.; Zhao, J. *Chem. Sci.* **2012**, *3*, 2920.
- (33) Cao, X.; Lin, W.; Zheng, K.; He, L. *Chem. Commun.* **2012**, *48*, 10529.
- (34) Liu, T.; Xu, Z.; Spring, D. R.; Cui, J. *Org. Lett.* **2013**, *15*, 2310.
- (35) Liu, T.; Zhang, X.; Qiao, Q.; Zou, C.; Feng, L.; Cui, J.; Xu, Z. *Dyes Pigments* **2013**, *99*, 537.
- (36) Liu, Y.; Feng, G. *Org. Biomol. Chem.* **2014**, *12*, 438.
- (37) Liu, C.; Peng, B.; Li, S.; Park, C.-M.; Whorton, A. R.; Xian, M. *Org. Lett.* **2012**, *14*, 2184.
- (38) Wang, B.; Li, P.; Yu, F.; Chen, J.; Qu, Z.; Han, K. *Chem. Commun.* **2013**, *49*, 5790.
- (39) Zhou, G.; Wang, H.; Ma, Y.; Chen, X. *Tetrahedron* **2013**, *69*, 867.

- (40) Mao, G.-J.; Wei, T.-T.; Wang, X.-X.; Huan, S.-y.; Lu, D.-Q.; Zhang, J.; Zhang, X.-B.; Tan, W.; Shen, G.-L.; Yu, R.-Q. *Anal. Chem.* **2013**, *85*, 7875.
- (41) Saha, T.; Kand, D.; Talukdar, P. *Org. Biomol. Chem.* **2013**, *11*, 8166.
- (42) Sun, W.; Fan, J.; Hu, C.; Cao, J.; Zhang, H.; Xiong, X.; Wang, J.; Cui, S.; Sun, S.; Peng, X. *Chem. Commun.* **2013**, *49*, 3890.
- (43) Zhang, L.; Li, S.; Hong, M.; Xu, Y.; Wang, S.; Liu, Y.; Qian, Y.; Zhao, J. *Org. Biomol. Chem.* **2014**, *12*, 5115.
- (44) Jiang, Y.; Wu, Q.; Chang, X. *Talanta* **2014**, *121*, 122.
- (45) Bae, S. K.; Heo, C. H.; Choi, D. J.; Sen, D.; Joe, E.-H.; Cho, B. R.; Kim, H. M. *J. Am. Chem. Soc.* **2013**, *135*, 9915.
- (46) Wu, Z.; Li, Z.; Yang, L.; Han, J.; Han, S. *Chem. Commun.* **2012**, *48*, 10120.
- (47) Kand, D.; Mandal, P. S.; Datar, A.; Talukdar, P. *Dyes Pigments* **2014**, *106*, 25.
- (48) Volmajer, J.; Toplak, R.; Leban, I.; Marechal, A. M. L. *Tetrahedron* **2005**, *61*, 7012.
- (49) Belkheira, M.; El Abed, D.; Pons, J.-M.; Bressy, C. *Chem. Eur. J.* **2011**, *17*, 12917.

Appendix

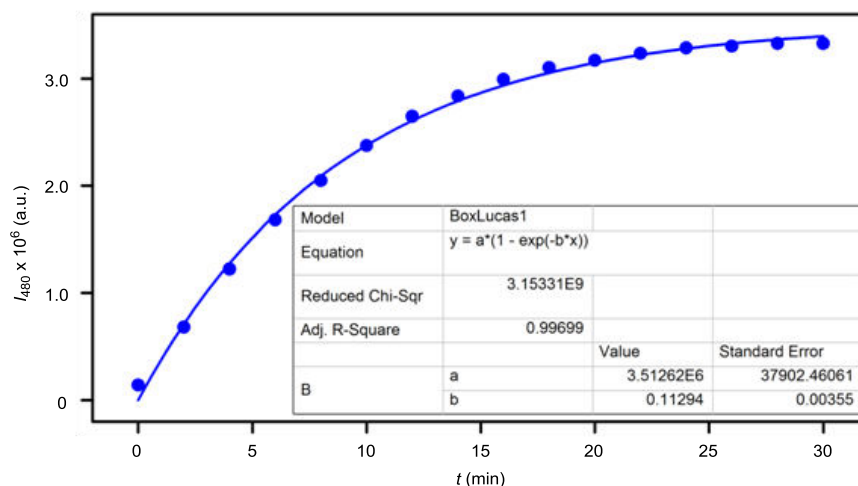


Figure 20. Fluorescent intensities recorded with time at 480 nm when probe **36** was treated with 150 μM of Na_2S .

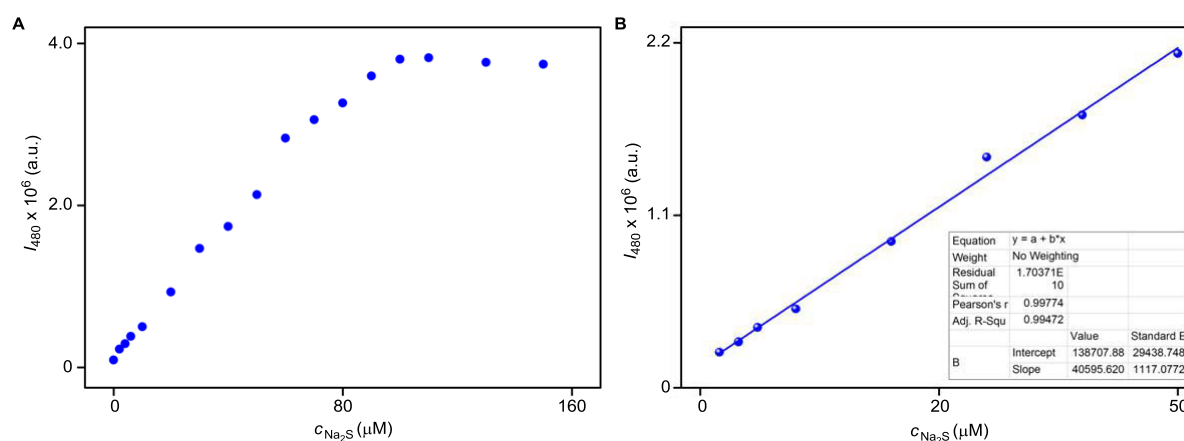


Figure 21. Fluorescence intensity at 480 nm I_{480} versus concentration of Na_2S $c_{\text{Na}_2\text{S}}$ plot (A). Representation of the linear region of the plot and determination of the slope of the linear plot (B).

NMR spectra:

190514-10-PKM-02-05

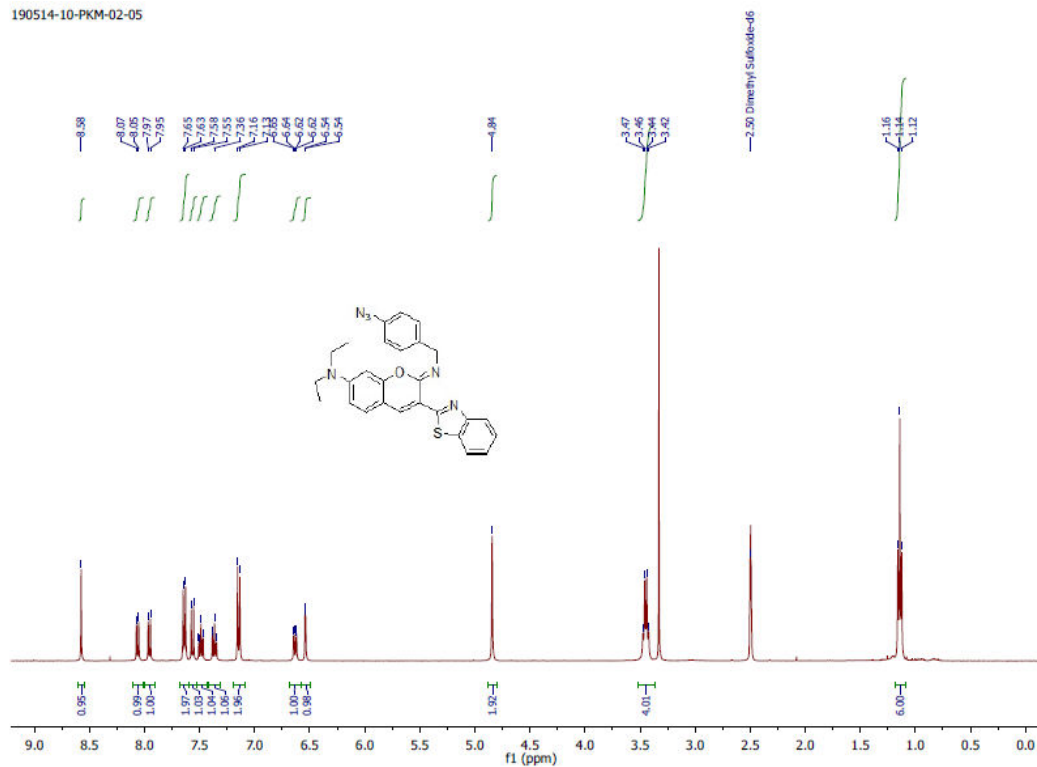


Figure 22. ^1H NMR spectra of **32** in DMSO-D_6 .

20150303-PKM-02-05-VT-90
PKM-02-05-VT-90

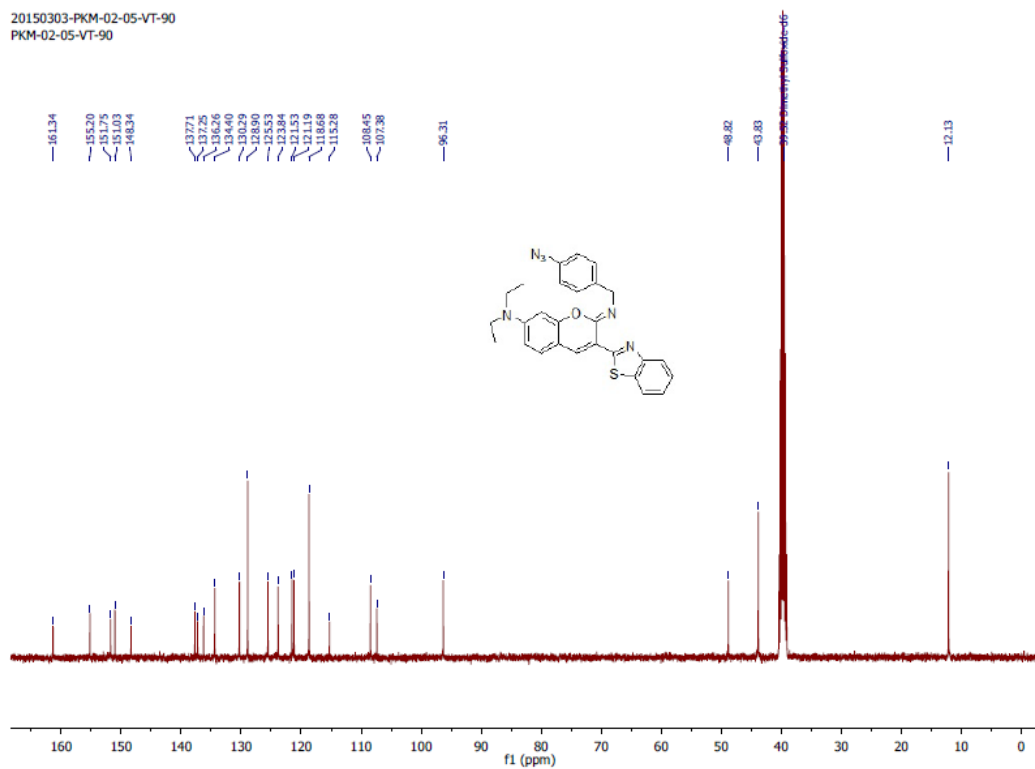


Figure 23. ^{13}C NMR spectra of **32** in DMSO-D_6 .

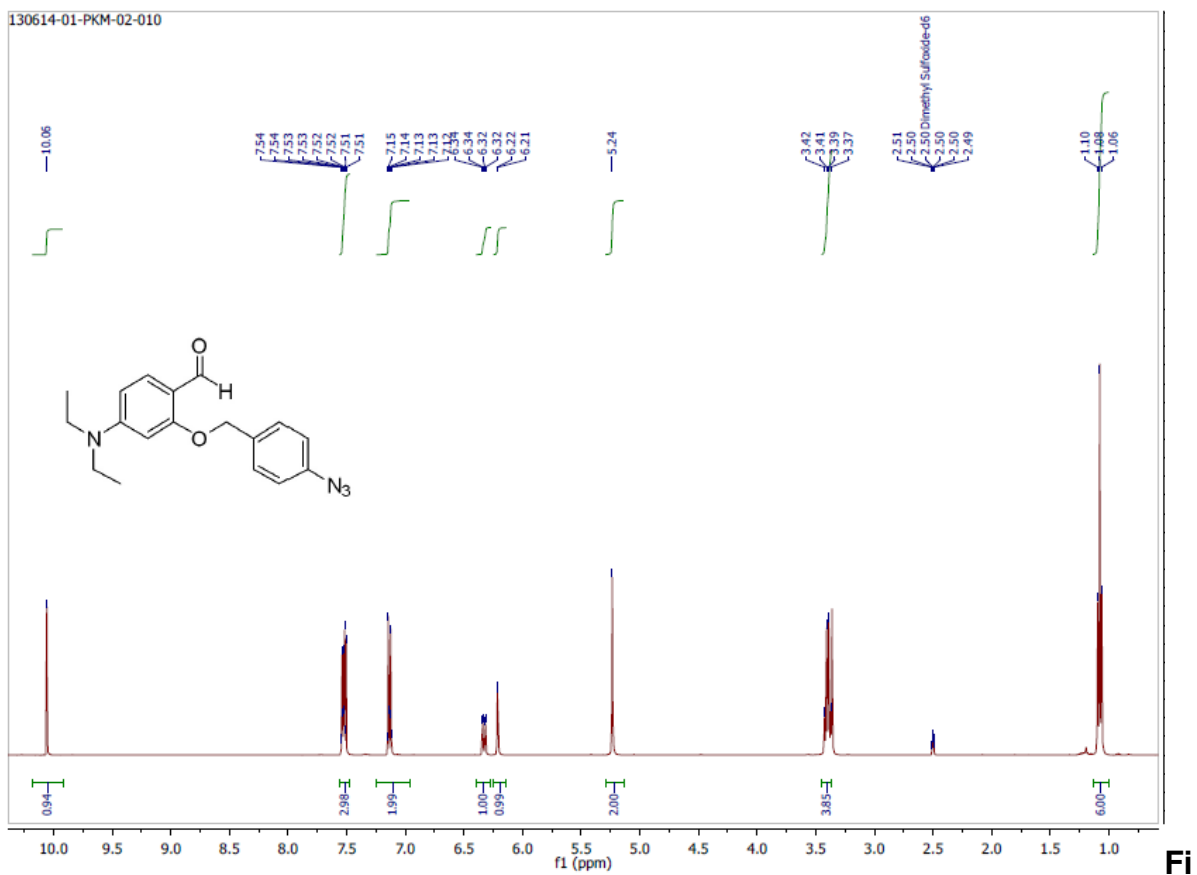


Figure 24. ^1H NMR spectra of **43** in DMSO-D_6 .

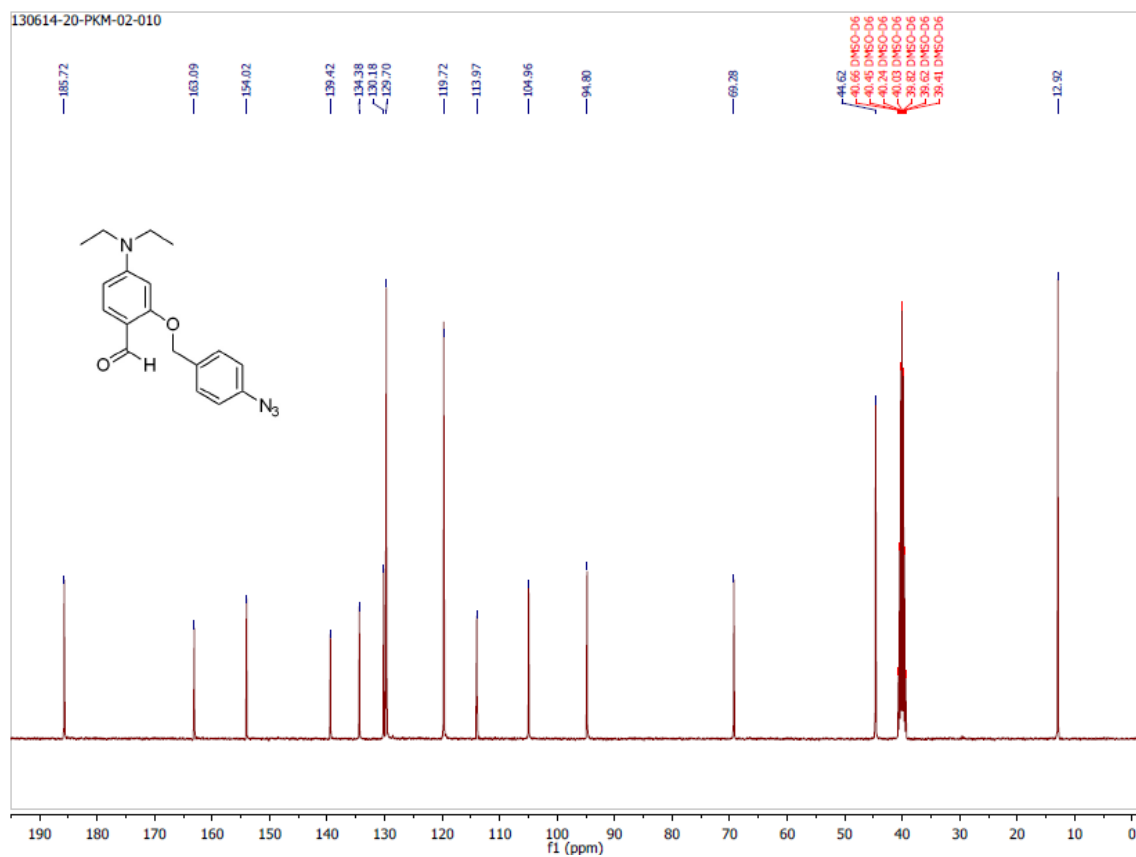


Figure 25. ^{13}C NMR spectra of **43** in DMSO-D_6 .

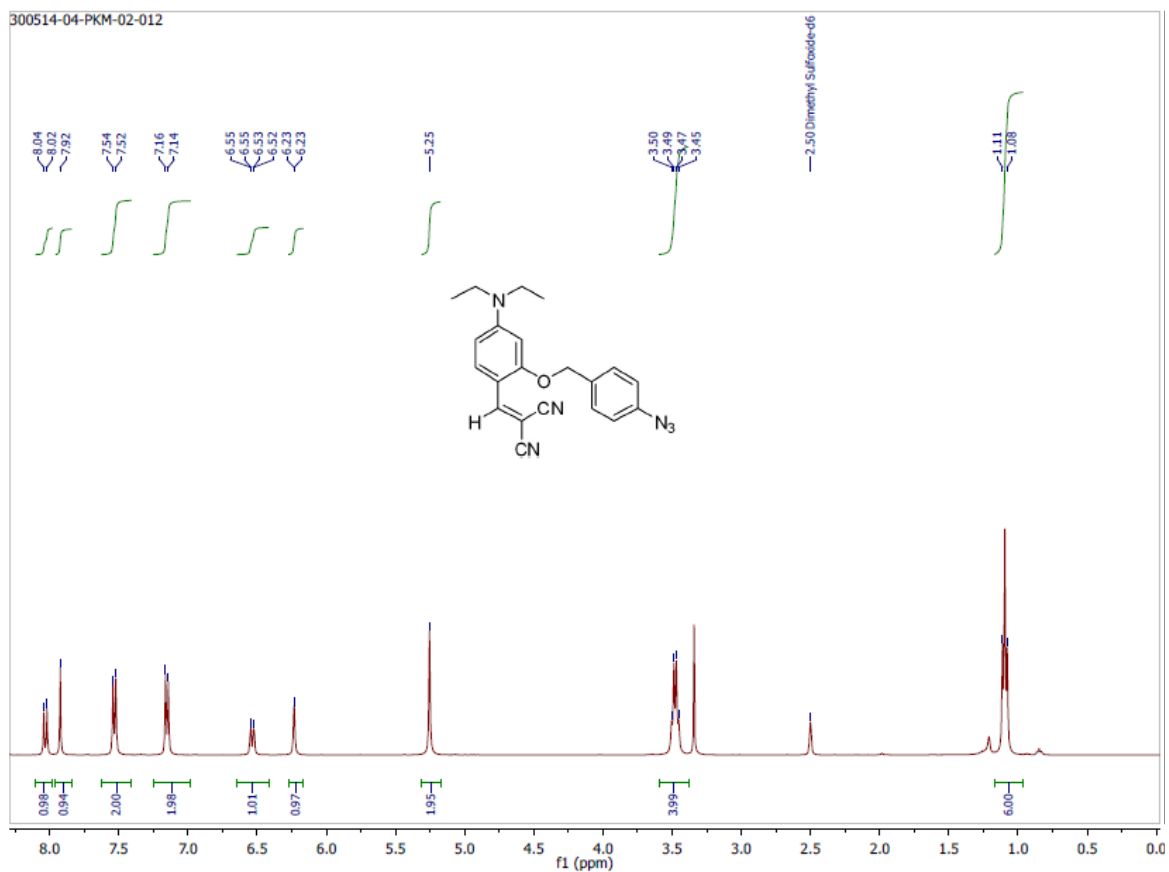


Figure 26. ¹H NMR spectra of **36** in DMSO-D₆.

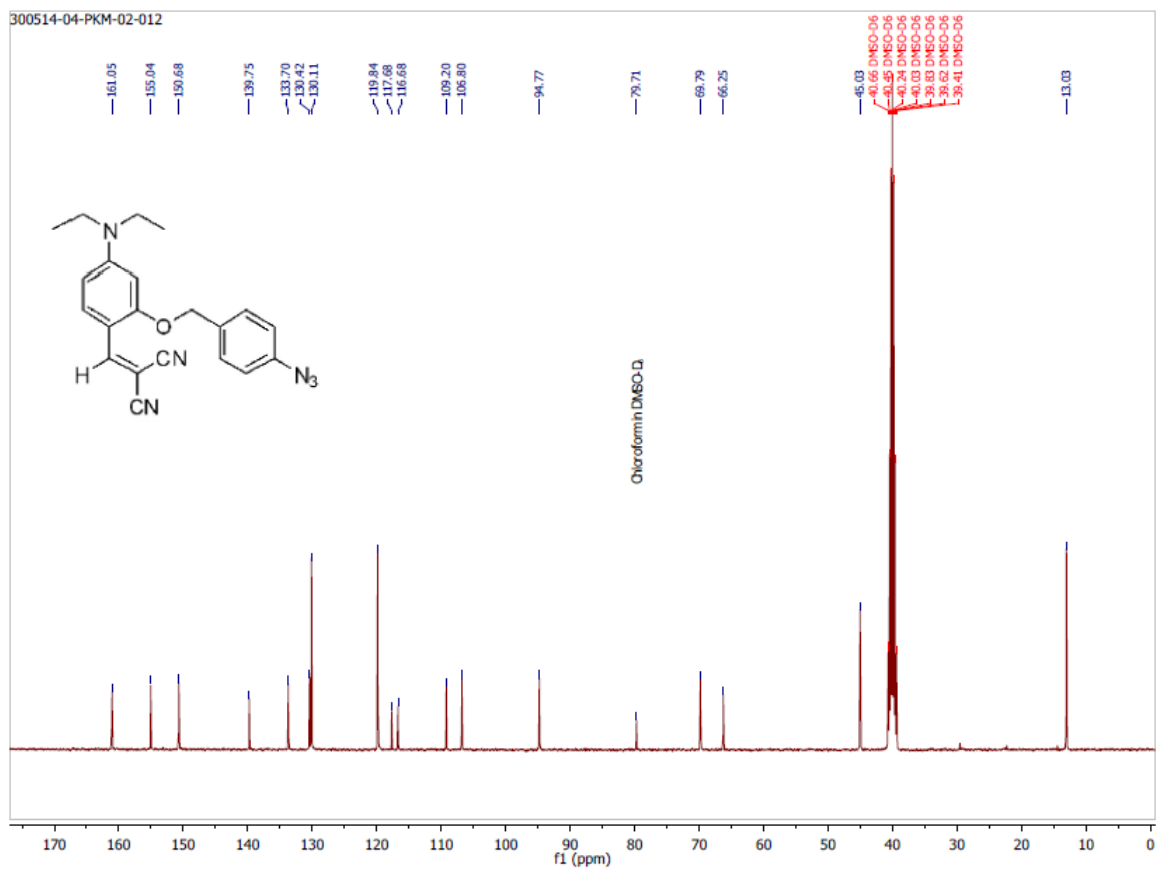


Figure 27. ¹³C NMR spectra of **36** in DMSO-D₆.

Crystal Data.

Crystal structure Parameters:

The compound was crystallized from DMSO at room temperature. Single-crystal X-ray data of compound **36** was collected at 200 K on a Bruker KAPPA APEX II CCD Duo diffractometer (operated at 1500 W power: 50 kV, 30 mA) using graphite-monochromated Mo K α radiation ($\lambda = 0.71073$ Å).

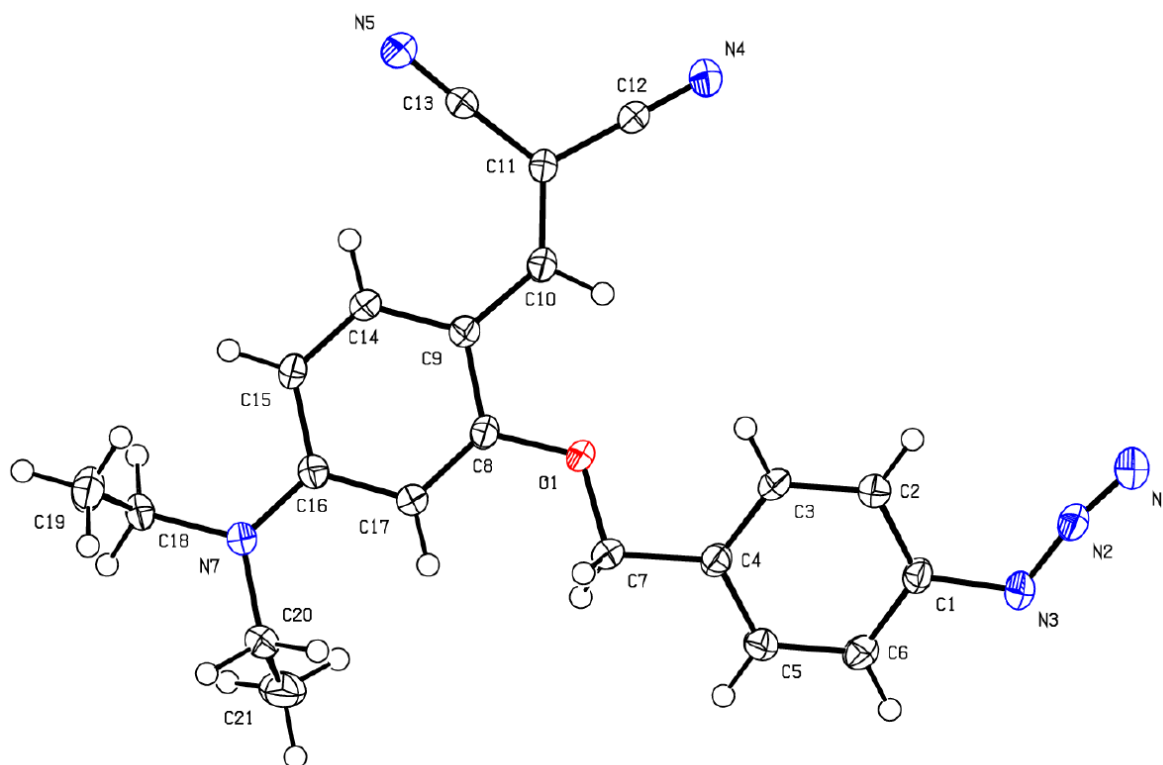


Figure 28. ORTEP diagram of probe **36**.

HPLC Chromatogram.

Conditions:

Column: Agilent Eclipse plus 5 μ m

Flow: 1.0 mL/min

Method: Gradient

60 % Acetonitrile/water 0 min

60 % Acetonitrile 0 to 05 min

90 % Acetonitrile 05 to 25 min

Wavelength: 440 nm.

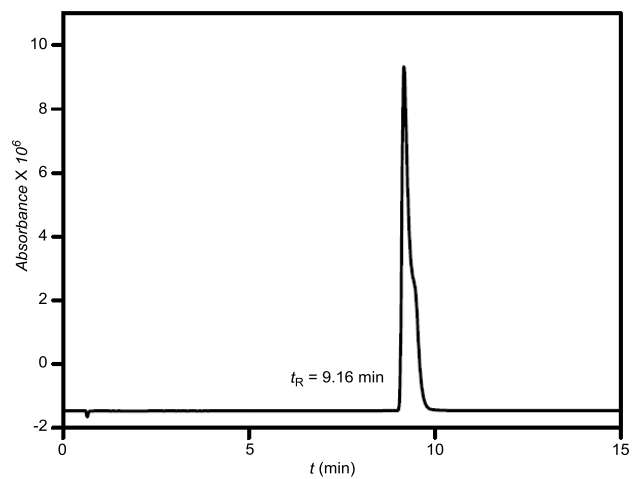


Figure 29. HPLC chromatogram of pure probe **36** (100 μ M).

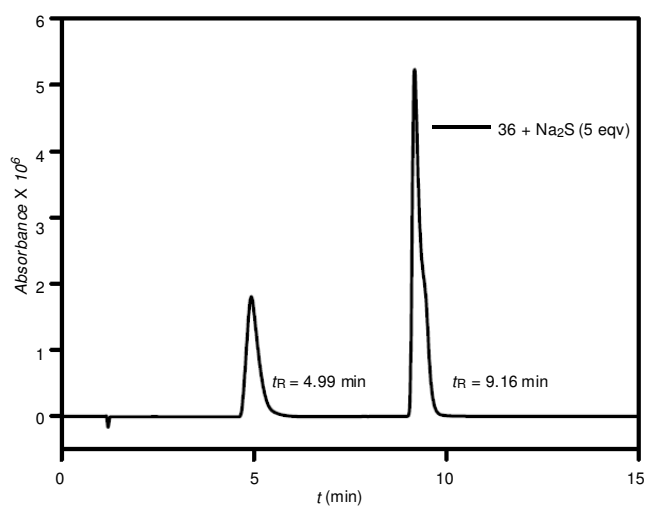


Figure 30. HPLC chromatogram of the reaction mixture containing probe **36** + Na₂S (5 equiv), recorded after 20 min.

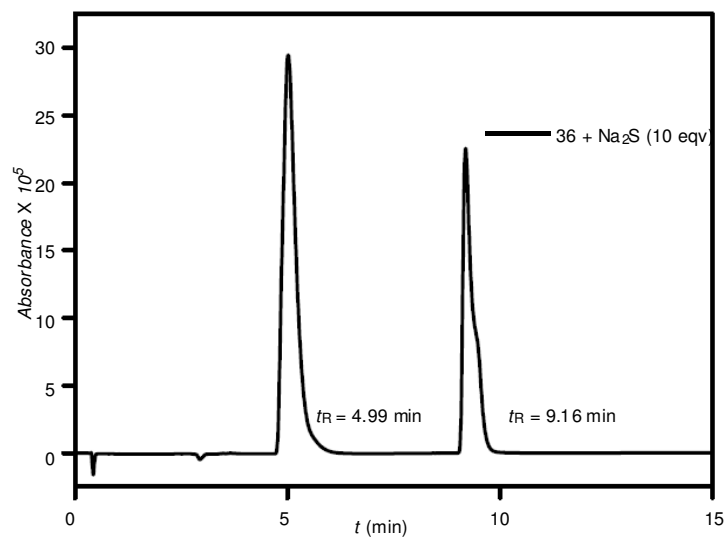


Figure 31. HPLC chromatogram of the reaction mixture containing probe **36** + Na₂S (10 equiv), recorded after 20 min.

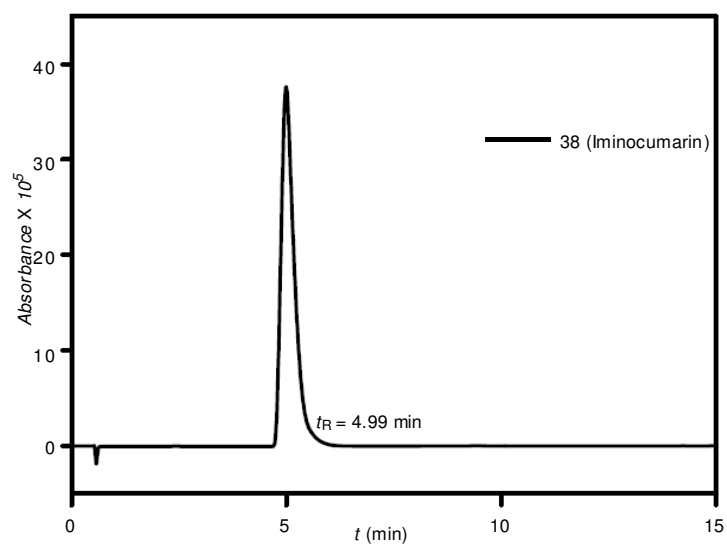


Figure 32. HPLC chromatogram of pure iminocoumarin **38** (100 μ M).